

INFORMATION TO USERS

This manuscript has been reproduced from the microfilm master. UMI films the text directly from the original or copy submitted. Thus, some thesis and dissertation copies are in typewriter face, while others may be from any type of computer printer.

The quality of this reproduction is dependent upon the quality of the copy submitted. Broken or indistinct print, colored or poor quality illustrations and photographs, print bleedthrough, substandard margins, and improper alignment can adversely affect reproduction.

In the unlikely event that the author did not send UMI a complete manuscript and there are missing pages, these will be noted. Also, if unauthorized copyright material had to be removed, a note will indicate the deletion.

Oversize materials (e.g., maps, drawings, charts) are reproduced by sectioning the original, beginning at the upper left-hand corner and continuing from left to right in equal sections with small overlaps.

ProQuest Information and Learning
300 North Zeeb Road, Ann Arbor, MI 48106-1346 USA
800-521-0600

UMI[®]

University of Alberta

**Characterization of functionalized aryl layers on carbon electrodes
deposited from aqueous solutions**

by

Bushra Sajed



A thesis submitted to the Faculty of Graduate Studies and Research in partial
fulfillment of the requirements for the degree of Master of Science

Department of Chemistry

Edmonton, Alberta

Spring 2005



Library and
Archives Canada

Bibliothèque et
Archives Canada

0-494-08146-5

Published Heritage
Branch

Direction du
Patrimoine de l'édition

395 Wellington Street
Ottawa ON K1A 0N4
Canada

395, rue Wellington
Ottawa ON K1A 0N4
Canada

Your file *Votre référence*

ISBN:

Our file *Notre référence*

ISBN:

NOTICE:

The author has granted a non-exclusive license allowing Library and Archives Canada to reproduce, publish, archive, preserve, conserve, communicate to the public by telecommunication or on the Internet, loan, distribute and sell theses worldwide, for commercial or non-commercial purposes, in microform, paper, electronic and/or any other formats.

The author retains copyright ownership and moral rights in this thesis. Neither the thesis nor substantial extracts from it may be printed or otherwise reproduced without the author's permission.

AVIS:

L'auteur a accordé une licence non exclusive permettant à la Bibliothèque et Archives Canada de reproduire, publier, archiver, sauvegarder, conserver, transmettre au public par télécommunication ou par l'Internet, prêter, distribuer et vendre des thèses partout dans le monde, à des fins commerciales ou autres, sur support microforme, papier, électronique et/ou autres formats.

L'auteur conserve la propriété du droit d'auteur et des droits moraux qui protègent cette thèse. Ni la thèse ni des extraits substantiels de celle-ci ne doivent être imprimés ou autrement reproduits sans son autorisation.

In compliance with the Canadian Privacy Act some supporting forms may have been removed from this thesis.

Conformément à la loi canadienne sur la protection de la vie privée, quelques formulaires secondaires ont été enlevés de cette thèse.

While these forms may be included in the document page count, their removal does not represent any loss of content from the thesis.

Bien que ces formulaires aient inclus dans la pagination, il n'y aura aucun contenu manquant.


Canada

Dedicated to my husband

and to my mother...

Abstract

In this work, functionalized aryl films were deposited from aqueous solutions on carbon surfaces by diazonium reduction method and were characterized by electrochemical method and atomic force microscopy (AFM). The films deposited from aqueous solutions are compared to those obtained from organic solution, which is more commonly used as a deposition medium.

Initially, two types of carbon electrodes, namely polished glassy carbon (GC) and pyrolyzed photoresist film (PPF) electrodes were modified with aryl films from aqueous acid solution. The films effectively blocked electron transfer to solution bound redox species. Later GC electrodes were modified with aryl layers from a variety of aqueous solutions with a range of pH. The results showed that aryl groups formed blocking films when deposited from acidic to neutral pH solutions. Incomplete films were formed in basic solution, probably due to the fact that aryl diazonium ions react chemically with basic solution and hence are less available to be reduced to the aryl radical. UV-VIS spectra of diazoniums in different supporting electrolytes also supported these results.

For AFM study of aryl films, carbon film electrodes prepared by electron-beam evaporation (ECF) were used as substrates. The ECF electrodes were patterned using photolithography. These patterned ECF electrodes provided a reliable platform for measuring the thickness of aryl films with AFM. The thickness of aryl films deposited electrochemically from organic solution were higher than those deposited from aqueous acid solution. This may be due to the higher diffusion coefficient of diazoniums in organic medium as compared to the

aqueous acid medium. The self-assembly of aryl groups on carbon surface from diazonium salt solutions was also investigated.

Acknowledgements

All praise belongs to Almighty Allah, the most Beneficent and the most Merciful.

I like to thank several people without whose assistance my academic life and preparation of this thesis would not have been possible. My sincere appreciation goes to my supervisor, Dr. Mark McDermott. Your guidance, advice and encouragement were the driving force behind this work. Your encouraging words even after a small task always made me feel positive. The time I spent in your group was an enjoyable experience and your assistance in areas outside the academic sphere is greatly appreciated.

I wish to thank all the current McDermott group members, Francis, Aaron, Dwayne, Chris, Rongbing and Hongmei for your assistance and advice in both academic and non-academic pursuits. I also thank former group members, Solomon, Vishal, Abbas, James, Beatrice and Salome for your help and useful discussions.

I thank Department of Chemistry for financial support and NSERC for funding our research. I am indebted to the members of my M.Sc. committee for their time and useful comments. I thank the entire faculty and staff in Chemistry Department, specially, Ilona Baker and Dr. Norman Gee for your assistance. I like to thank the following persons: Dr. Arthur Mar (Department of Chemistry), for the use of furnace, Greg Popowich (Department of Physics), for preparation of

ECF substrates, staffs in Nanofab, University of Alberta and Spectral Services laboratory of Chemistry Department.

I wish to thank my previous supervisors, Dr. Muhibur Rahman and Dr. Yousuf A. Mollah of Department of Chemistry, University of Dhaka, Bangladesh, for their encouragement and support towards higher studies in Canada. Last but not the least, I thank my husband Rashed, whose love, support, patience and endless assistance made this thesis possible. I am greatly indebted to all my family members for their constant support and prayers. I like to specially thank my mother for grooming me up to I'm today and letting me pursue my dreams. Finally I thank all my friends at home and abroad for remaining true friends for life.

Table of Contents

Chapter I: Introduction

Carbon Electrodes	1
Chemically Modified Carbon Electrodes	5
Modification of Carbon Electrodes by Reduction of Diazonium Salts	9
Electron transfer Blocking Studies	16
Research Objectives	20
References	21

Chapter II: Deposition of Functionalized Aryl Groups on Carbon Electrodes from Aqueous Solutions

Introduction	26
Experimental Section	28
Results and Discussion	30
Conclusions	61
References	61

Chapter III: Study of Functionalized Aryl Layers on Carbon Substrates with Atomic Force Microscopy

Introduction	64
Experimental Section	65
Results and Discussion	68
Conclusions	89
References	90

Chapter IV: Conclusions and Future Work

Overall Conclusions	93
Suggestions for future work	95
References	96

List of Tables

Table 2.1	Results from electrochemical studies on GC electrodes.	39
Table 2.2	Results from electrochemical studies on pyrolyzed photoresist film (PPF) surface.	45
Table 2.3	Results of UV-VIS spectra of diazoniums in different supporting electrolytes.	60
Table 3.1	Average thickness of electrochemically deposited aryl layers measured with AFM.	77
Table 3.2	Average thickness of self-assembled nitrophenyl layers measured with AFM.	87

List of Figures

Figure 1.1	Structures of (A) highly oriented pyrolytic graphite (HOPG) and (B) glassy carbon (GC).	2
Figure 2.1	Cyclic voltammograms for the reduction of 2.5 mM NB from 0.1 M H ₂ SO ₄ on GC.	31
Figure 2.2	Effect of number of deposition cycles of NB (0.1 M H ₂ SO ₄) on blocking of GC surface shown with the voltammetry of 1 mM Fe(CN) ₆ ^{3-/4-} (1 M KCl).	33
Figure 2.3	Effect of number of deposition cycles of NB (0.1 M H ₂ SO ₄) on blocking of GC surface shown with the voltammetry of 1 mM Ru(NH ₃) ₆ ^{3+/2+} (1 M KCl).	35
Figure 2.4	Effect of number of deposition cycles of NB (0.1 M H ₂ SO ₄) on blocking of GC surface shown with the voltammetry of 5 mM Eu(NO ₃) ₃ ^{3+/2+} (0.2 M NaClO ₄).	36
Figure 2.5	Cyclic voltammograms for the reduction of 2.5 mM NB from (0.1 M Bu ₄ NBF ₄ +CH ₃ CN) on a GC surface.	38
Figure 2.6	Effect of number of deposition cycles of NB (0.1 M Bu ₄ NBF ₄ +CH ₃ CN) on blocking of GC surface shown with the voltammetry of 1 mM Fe(CN) ₆ ^{3-/4-} (1 M KCl).	40
Figure 2.7	Effect of number of deposition cycles of NB (0.1 M Bu ₄ NBF ₄ +CH ₃ CN) on blocking of GC surface shown with the voltammetry of 5 mM Eu(NO ₃) ₃ ^{3+/2+} (0.2 M NaClO ₄).	42
Figure 2.8	Cyclic voltammograms for the reduction of 2.5 mM NB from 0.1 M H ₂ SO ₄ on a PPF surface.	43
Figure 2.9	Cyclic voltammograms for the reduction of 2.5 mM NB from (0.1 M Bu ₄ NBF ₄ +CH ₃ CN) on a PPF surface.	44
Figure 2.10	Voltammetry of 1 mM DA (0.1 M H ₂ SO ₄) on GC surfaces modified with NB from solutions of various pH.	49
Figure 2.11	Cyclic voltammograms for the reduction of 5 mM PAA from (0.1 M Bu ₄ NBF ₄ +CH ₃ CN) on a GC surface.	51

Figure 2.12	Voltammetry of 1 mM DA (0.1 M H ₂ SO ₄) on GC surfaces modified with PAA from solutions of various pH.	52
Figure 2.13	Cyclic voltammograms for the reduction of 1 mM BP from (0.1 M Bu ₄ NBF ₄ +CH ₃ CN) on a GC surface.	54
Figure 2.14	Voltammetry of 1 mM DA (0.1 M H ₂ SO ₄) on GC surfaces modified with BP from solutions of various pH.	55
Figure 2.15	UV-VIS spectra of NB in different supporting electrolytes.	57
Figure 2.16	UV-VIS spectra of BP in different supporting electrolytes.	58
Figure 2.17	UV-VIS spectra of PAA in different supporting electrolytes.	59
Figure 3.1	(A) Contact mode topographic image of an unmodified ECF substrate. (B) Tapping mode topographic image of an ECF substrate modified by two potential cycles in 2.5 mM NB(0.1M Bu ₄ NBF ₄ + CH ₃ CN).	70
Figure 3.2	Cyclic voltammograms for the reduction of 2.5 mM NB from (0.1 M Bu ₄ NBF ₄ +CH ₃ CN) on (A) unpatterned (B) patterned ECF surface.	71
Figure 3.3	Tapping mode images of a patterned ECF substrate modified by 2 cycles in 2.5 mM NB(0.1 M H ₂ SO ₄). (A) Topographic image (B) Phase contrast image (C) Average section analysis performed on the topographic image (D) Corresponding cross-sectional profile.	73
Figure 3.4	(A) Topographic AFM image of a patterned ECF substrate modified with 10 deposition cycles in 2.5 mM NB(0.1M Bu ₄ NBF ₄ + CH ₃ CN) (B) Cross-sectional profile.	75
Figure 3.5	Tapping mode AFM images of a patterned ECF substrate modified by 2 cycles in 1 mM BP (0.1M Bu ₄ NBF ₄ + CH ₃ CN). (A) Topographic image (B) Corresponding phase contrast image (C) Cross-sectional profile.	78

Figure 3.6	(A) 14.4 X 14.4 μm topographic AFM image of a patterned ECF substrate modified by 2 cycles in 1 mM BP (0.1M $\text{Bu}_4\text{NBF}_4 + \text{CH}_3\text{CN}$) (B) A higher magnification image of the biphenyl film.	79
Figure 3.7	Comparison of peak current for the deposition of 2.5 mM NB from aqueous and organic medium on ECF surface.	81
Figure 3.8	Electrolysis experiment of NB in aqueous and organic medium.	83
Figure 3.9	Current vs. $t^{-1/2}$ plot for electrolysis of NB in organic and aqueous acid medium.	83
Figure 3.10	(A) Tapping mode topographic image of a patterned ECF substrate immersed in 2.5 mM NB((0.1M $\text{Bu}_4\text{NBF}_4 + \text{CH}_3\text{CN}$) for 1 hour (B) Cross-sectional profile.	86
Figure 3.11	(A) Tapping mode topographic image of a patterned ECF substrate immersed overnight in 2.5 mM NB(0.1 M H_2SO_4). (B) Cross-sectional profile.	88

List of Symbols

L_a	Intraplanar microcrystallite size
L_c	Interplanar microcrystallite size
d_{002}	Intraplanar spacing
D_O	Diffusion coefficient for oxidized species
D_R	Diffusion coefficient for reduced species
α	Transfer coefficient
v	Scan rate
k^0	Standard heterogeneous rate constant
ψ	Rate parameter
ΔE_p	Separation of cathodic and anodic peak potential
β	Tunneling parameter
A_{max}	Absorbance maxima
$\Delta\phi$	Phase angle shift
i_D	Diffusion current
i_p	Peak current in a cyclic voltammogram
F	Faraday's constant
A	Electrode area
C^*	Bulk concentration
n	Number of electrons

List of Abbreviations

AFM	Atomic force microscopy
BP	4-biphenyl diazonium tetrafluoroborate
BP _{ACN}	4-biphenyl film deposited from acetonitrile solution
BP _{AQ}	4-biphenyl film deposited from aqueous solution
BSA	Bovine serum albumin
Bu ₄ NBF ₄	Tetrabutylammonium tetrafluoroborate
CH ₃ CN	Acetonitrile
CV	Cyclic voltammetry
DA	Dopamine
DEA	Diethylaniline
ECF	e-beam deposited carbon film
ET	Electron transfer
GC	Glassy carbon
HOPG	Highly oriented pyrolytic graphite
IRRAS	Infrared reflectance absorption spectroscopy
NADH	Nicotinamide adenine dinucleotide
NB	4-nitrobenzene diazonium tetrafluoroborate
NHS	N-hydroxysuccinimide
NP	4-nitrophenyl
NP _{ACN}	4-nitrophenyl film deposited from acetonitrile solution
NP _{AQ}	4-nitrophenyl film deposited from aqueous solution
PAA	4-phenylacetic acid tetrafluoroborate

PAN	Poly acrylonitrile
PBS	Phosphate buffered saline
PPF	Pyrolyzed photoresist film
RBS	Rutherford backscattering
SECM	Scanning electrochemical microscopy
SEM	Scanning electron microscopy
SFM	Scanning force microscopy
UV-VIS	Ultraviolet-visible region of light
XPS	X-ray photoelectron spectroscopy

Chapter I

Introduction

Carbon Electrodes

Graphitic carbon is used extensively as an electrode material because of its wide potential window, low cost, good mechanical stability and compatibility with a variety of electrolytes. In addition, carbon materials can be produced in a variety of structures, such as powders, fibers, large blocks, thin solid and porous sheets. Their widespread utilization in electrosynthesis, electroanalysis and energy conversion has been reviewed [1-5].

The bulk properties of different types of sp^2 hybridized carbon vary greatly due to the size and orientation of graphitic crystallites [2]. The microcrystallite size of sp^2 hybridized carbon can be described by three independent variables. These are: intraplanar microcrystallite size (L_a), interplanar microcrystallite size (L_c) and intraplanar spacing (d_{002}). Figure 1.1A is an illustration of highly ordered pyrolytic graphite defining the crystallographic variables in sp^2 carbon. In short, L_a is the mean size of the graphitic microcrystallite along the basal plane, L_c is a measure of the thickness of the stacked graphitic layers and d_{002} is the X-ray diffraction designation corresponding to the distance between the layer planes. The main structural variables that affect electrochemical performance of different carbon surfaces include distribution of edge and basal plane sites, surface roughness, physically adsorbed impurities and chemisorbed species [2]. Carbon surfaces have a tendency to form covalent bonds (chemisorb) with a variety of

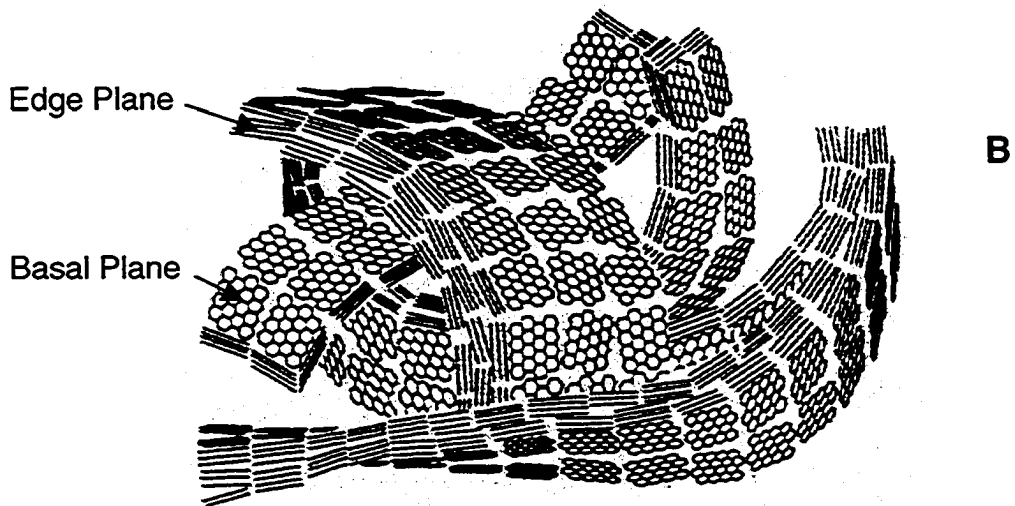
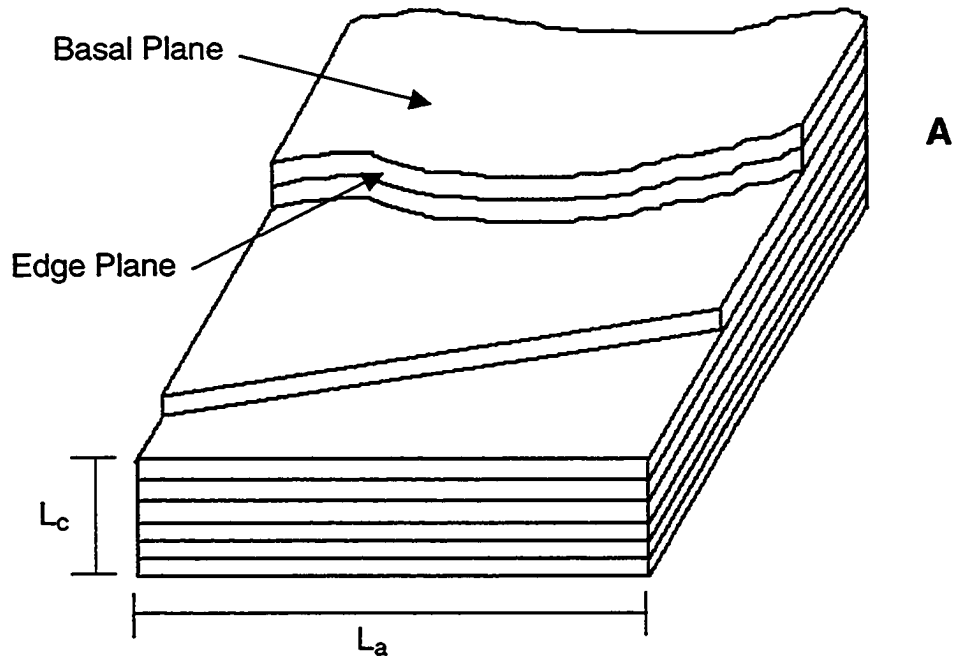


Figure 1.1: Structures of (A) highly oriented pyrolytic graphite (HOPG) and (B) glassy carbon (GC).

species, particularly oxygen containing groups, such as, phenol, carbonyl, carboxylic acid and quinones. These surface oxides play a large role in carbon surface chemistry.

Some of the commonly used carbon materials in electrochemistry include carbon black, glassy carbon (GC), single crystal graphite, highly oriented pyrolytic graphite (HOPG) and carbon fibers. The properties of GC and carbon films prepared by pyrolysis of photoresists and electron beam evaporation will be discussed next, as these were used in the research in this thesis.

Glassy carbon is a hard, solid carbon material that exhibits fracture behaviour similar to that of glasses. GC is made from polymeric resins such as polyacrylonitrile (PAN) or phenol/formaldehyde resin etc. The polymers are initially heated to 600-800 °C, which volatilize most of the noncarbon elements. The original polymeric backbone stays largely intact and prevents the formation of extensive graphitic domains [2]. Next, the material is heated slowly under pressure to 1000°C (GC-10), 2000°C (GC-20) or 3000°C (GC-30). Only small graphitic domains are formed even at 3000 °C and the material resembles a complex structure of interwoven graphitic ribbons, as shown in Fig. 1.1B. The manufacture and physiochemical properties of GC have been studied extensively by Jenkins and Kawamura [6]. GC-10 has somewhat irreproducible electrochemical properties and GC-30 often contains small bubbles formed during heat treatment [3]. Thus GC-20 is the most widely used material, which has also been used in our research. GC is impermeable to liquids and gases, polishable, can be exposed to heat, high vacuum, chemical derivatization and is

compatible with all common solvents. These properties have led to its widespread use in voltammetry and mechanistic electrochemistry.

Electrodes based on films of conducting material have been increasingly used in electrochemical experiments in recent years. Carbon films have been prepared by pyrolysis [7-10], vacuum evaporation [11, 12], sputtering [13], screen printing [14, 15] and laser photoactivation [16]. The fabrication of carbon films by pyrolyzing photoresist was first reported by Lyons *et. al.* [17]. One advantage of using photoresists as the starting materials is the ability to use photolithography to make carbon electrode devices. Electrochemical properties of pyrolyzed photoresist films (PPF) were studied by several groups [18-20]. The surface structure of the films has been characterized by scanning electron microscopy (SEM), atomic force microscopy (AFM), Raman spectroscopy, X-ray photoelectron spectroscopy (XPS), while the electrochemical properties have been investigated mainly by cyclic voltammetry [19, 20]. The properties of the film surface are similar to a "near atomically flat" version of GC, but with some differences in surface chemistry. The oxygen/carbon (O/C) atomic ratio of PPF is low (~1% for 1100°C pre-treatment) and increases more slowly upon exposure to air than that for GC, treated under identical conditions. The pyrolyzed films have low capacitance and background current, about one-fourth of that observed on GC. The physisorption of methylene blue and anthraquinone -2,6- disulfonate (AQDS) is weaker on PPF than on polished or heat-treated GC. Electron transfer rates are slightly slower for outer-sphere redox systems on PPF, but much slower for systems dependent on surface oxides or adsorption.

The preparation of carbon films by electron-beam (e-beam) evaporation was first reported by Mattson *et. al.* [21]. Recently the fabrication of high-purity carbon films using e-beam evaporation on highly doped silicon wafers has been reported by our group [22]. The microstructure, roughness and electrochemical activity of these carbon thin films were characterized. Pyrolyzed films exhibit electron transfer rates comparable to GC but have slightly higher roughness than the nonpyrolyzed films. Nonpyrolyzed films possess near atomic-scale flatness. These easily-prepared, ultra-flat films can be utilized in molecular electronics and AFM studies.

Chemically Modified Carbon Electrodes

Modification of carbon surfaces has been the subject of numerous studies in the last three decades because of their potential application in catalysis, corrosion protection, analytical purposes and biotechnology. Methods for the covalent attachment of molecules to carbon surfaces can be divided into two categories: Derivatization of existing functional groups and covalent attachment directly to the carbon backbone via a carbon-carbon bond. These methods will be discussed in the current section. The modification of carbon surface by electrochemical reduction of diazonium salts will be discussed in a separate section.

The principle of covalently modified electrodes was first demonstrated by Watkins and coworkers [23]. They reported a method of binding optically active amino acids on to graphite via amide bonds, thereby forming a chiral electrode

surface to perform an asymmetric reduction. Thereafter, Elliott and Murray employed organosilane chemistry to prepare chemically modified GC and graphite electrodes with surface bound amine, ethylenediamine, pyridine and alkyl chloride groups [24]. The modified electrodes retained electrochemical activity toward solution redox reagents and were themselves electrochemically stable. The surface of GC can be oxidized to produce interfacial carbonyl or carboxyl groups. Lennox and Murray utilized the presence of these carboxyl groups to chemically modify electrodes. They used thionyl chloride activation of a thermally oxidized GC electrode to chemically bind a tetraphenylporphyrin ring on GC surface [25]. Due to the well-behaved non-aqueous solution electrochemistry of the ring, subsequent metallation of the immobilized porphyrin and similar molecular systems are known to exert potentially useful electrocatalytic effects.

Koval *et. al.* reported a procedure for attaching a ruthenium redox couple to graphite electrodes by coordinating the metal to a pyridine ligand which was, in turn, covalently linked to the graphite surface via amide bonds [26]. Cyclic voltammetry and differential pulse voltammetry were used to study the electrochemical behaviour of the attached complexes and to measure surface concentration.

Collman and coworkers reported the development of an electrode material that can catalyze the four-electron reduction of oxygen to water [27]. They synthesized a series of dimeric metalloporphyrin molecules in which the two porphyrin rings were constrained to lie parallel to one another by two amide bridges of varying length that linked the rings together. These cofacial

metalloporphyrins were then applied to the surface of graphite electrodes and all molecules showed some catalytic activity.

Evans and Kuwana investigated the formation of functional groups on carbon electrodes with radio-frequency plasma. The reactive plasma employed for modifying carbon surfaces included oxygen, ammonia and hydrogen bromide gases [28]. The physical and chemical consequences of the plasma treatments were investigated by cyclic voltammetry, capacitance measurements and X-ray photoelectron spectroscopy (XPS). The results indicated that the coverage of oxygen or nitrogen containing functional groups was enhanced by this process.

A novel route for modifying carbon fibres was investigated by Barbier *et. al.*, which was based on the electrooxidation of amine containing compounds [29]. The method proceeds via a one-electron oxidation of an amine functionality to its corresponding cation radical, which subsequently forms a carbon-nitrogen linkage at the carbon surface. They used this method for improving the toughness of carbon-epoxy composites. Park and Donnet have examined the effect of amine modification on the acid-base interactions between carbon fibers and an epoxy matrix [30]. Modification with ethylene diamine and triethylene tetraamine significantly increased the basicity of the fibers and strengthened their acid-base interaction with matrix. This, in turn, was reflected in increased interfacial shear strength of the composites. Adenier and coworkers have investigated the oxidation of aliphatic amines by cyclic voltammetry and preparative electrolysis [31]. They established the oxidation mechanisms and measured the lifetimes of the radical cations. They also studied the attachment of

amines to GC, Au and Pt electrodes and showed that the radical obtained after deprotonation reacts with the electrode surface, not the radical cation.

Electrochemical oxidation of amine containing compounds was utilized by Deinhammer and coworkers to modify GC electrodes [32]. They immobilized dopamine on the modified GC surface, which facilitated the oxidation of β -nicotinamide adenine dinucleotide (β -NADH). They also demonstrated the applicability of this method for the construction of biosensors that are based on biotin-avidin complexation. Downard and Mohamed utilized the method to prevent protein adsorption at GC electrodes [33]. Careful control of conditions for the oxidation of tetraethylene glycol diamine resulted in modified electrodes which were highly permeable to small redox probes but effectively excluded proteins from the surface.

Anne *et. al.* reported a facile and versatile method of modifying carbon surfaces by the reaction of N-hydroxysuccinimide (NHS) esters with freshly polished GC electrodes [34]. It was shown that the derivatization results from the formation of a covalent peptide linkage by reaction of the NHS ester with superficial amino groups on the GC surface. This strategy could be used to directly bind esters of biomolecules to the carbon surface.

Anodic oxidation of GC electrodes in 1° aliphatic alcohol (with H₂SO₄ or LiClO₄ as electrolytes) yields a layer of alkyl groups covalently attached to the electrode via an ether link [35, 36]. These modified GC surfaces have been used to suppress electrode fouling originating from adsorbed proteins in electrochemical measurements of biological fluids.

The oxidation of arylacetates in acetonitrile for modifying GC and basal plane HOPG has been reported [37]. Electrochemical oxidation of the corresponding carboxylates (Kolbe reaction), solidly attached a monolayer of aryl methyl groups on carbon surfaces. The easily accessible starting molecules and the presence of appropriate substituents on the phenyl rings makes this type of derivatization a convenient starting point for further chemical modifications.

Nowall and coworkers used different forms of microreagent mode of scanning electrochemical microscopy (SECM) to attach biotin on micron sized regions of a carbon electrode surface [38]. The SECM probe tip was used as an electrochemical pen to deposit biotin. This process can lead to the fabrication of biosensors that can be tailor-made for a variety of applications. Hayes and Kuhr attached biotin to a carbon fiber surface via reduction of biotin hydrazide in phosphate buffer pH 8.5 [39]. Although the nature of the surface attachment had not been characterized, but after considering the impact of modification on NADH voltammetry, it was concluded that reaction between the hydrazide and a surface carbonyl was not likely and a covalent bond with the carbon surface was a possibility. Thus electrolysis of hydrazides is a promising reaction to covalently attach monolayers.

Modification of Carbon Electrodes by Reduction of Diazonium Salts

Delamar and coworkers first reported a method for covalent attachment of aryl groups on carbon surfaces that involves electrochemical reduction of diazonium salts in acetonitrile solutions [40]. One-electron reduction of diazonium

salts form aryl radicals, which subsequently couple to the carbon surface. A large variety of functionalized aryl groups can be grafted by this method. Furthermore, once attached to the carbon surface, the functionalized aryl groups can be modified by classical chemical reactions. Hence the method presents a facile and versatile means to modify carbon electrodes. This thesis explores further expansion of this method. The current section will review some work on characterization and application of surfaces modified via this method.

Various forms of carbon have been modified via the diazonium reduction method including GC, edge and basal plane HOPG, carbon fiber and powder, carbon films and boron-doped diamond. The modified electrode surfaces have been characterized by XPS [40-44], Rutherford backscattering (RBS) [41], infrared reflectance absorption spectroscopy (IRRAS) [41, 45], Auger spectroscopy [41], unenhanced Raman spectroscopy [43, 44] and scanning probe microscopy (SPM) [41, 45, 46]. A comprehensive review by Downard summarizes the methods, scope and applications of electrochemically assisted, covalently modified carbon electrodes [47].

Electrodes modified by the reduction of diazonium salts have been found to be stable to long term storage in air and to sonication in various organic solvents [40, 41]. Auger electron spectroscopy showed peaks characteristic of N bonds for basal plane HOPG modified with 4-nitrophenyl groups even when heated to 700 K and disappeared only at 1400 K [41]. The stability can be attributed to the formation of a covalent bond between aryl group and the carbon surface. Raman spectroscopy provided evidence for freely rotating surface

groups, consistent with a single C-C bond between the surface and the modifier [48].

Allongue and coworkers analyzed the current-potential curves obtained during repetitive cyclic voltammetric (CV) scans at GC and basal plane HOPG in a solution of 4-nitrobenzene diazonium salt [41]. The CVs supported a mechanism in which all the radicals produced by reduction of the diazonium cations do not couple with the carbon surface. At basal plane HOPG, 56% of radicals react with the surface as compared to 84% at GC, while the remaining radicals escape into solution. This comparison indicates that edge plane carbon is more reactive towards coupling than basal plane.

Kariuki and McDermott explored the nucleation and growth of functionalized aryl films on HOPG [46]. Electrochemical and scanning probe microscopic techniques were utilized to track the development of diethylaniline (DEA) films. Their findings showed that initial nucleation of these films started at cleavage steps and continued deposition resulted in growth on the supposedly nonreactive basal plane. Nucleation on the basal plane occurred probably at atomic scale defect sites. The film growth occurred in both 2 and 3-dimensions through the binding of electrochemically generated aryl radicals to aryl groups already bound to the surface.

The derivatization of H-terminated GC via reduction of 4-nitrobenzene diazonium in acetonitrile has been reported [44]. Hydrogen radicals were generated by using a hot filament technique from a flow of hydrogen gas, which attacked GC surfaces. The modified surface had a low O/C ratio and presumably

surface C-H bonds. The proposed mechanism for nitrophenyl modification involves abstraction of an H-atom by a nitrophenyl radical forming a surface carbon radical and soluble nitrobenzene. This surface radical then couples with a second nitrophenyl radical to form the monolayer

Several workers have examined the reductive electrochemistry of 4-nitrophenyl modified electrodes in protic solvents [40, 41, 43, 49, 50]. Ortiz *et. al.* observed that, in addition to reduction of the nitro substituent to the amine, the intermediate NHOH/NO redox couple was also formed in aqueous acid [50]. XPS investigations indicated that only a fraction of the nitro groups were reduced. Simultaneous grafting of 4-nitrophenyl and reduction of the nitro substituent to an amine was possible when the modification was carried out with a sufficiently negative electrolysis potential in aqueous acid solutions (H_2SO_4 and HCl , $\text{pH}<2$) [49].

Phenylacetate modified electrodes were used for the immobilization of glucose oxidase on GC electrodes [51]. After grafting of the phenylacetate layer by reduction of the corresponding diazonium salt, the enzyme was coupled via amide bond formation. The authors noted that in contrast to the oxidative generation of carboxylate groups on GC surface, diazonium reduction does not lead to surface roughening and large background currents and should allow the design of customized enzyme linkages.

This approach has been utilized by Dequaire *et. al.* to attach p-benzoyl biocytin to screen-printed graphite electrodes by reduction of a diazonium derivative [52]. The modified electrodes were reacted with Extravidin followed by

biotinylated alkaline phosphatase. Biotinylated screen-printed electrodes could be regenerated by removal of avidin in a solution of guanidine hydrochloride, thus allowing reuse of the electrodes. These factors constitute a promising versatile platform for the construction of electrochemical biosensor arrays.

Delamar and coworkers used the diazonium reduction method to modify carbon surfaces which improved adhesion to epoxy resins [49]. Their strategy involved modifying the carbon surface with aminophenyl or phenol groups followed by reaction with epoxy resins. The mechanical properties of carbon-epoxy composites prepared from modified carbon fibers were compared with those prepared from untreated fibers. The debonding shear stress increased after modification indicating improved adhesion.

GC surface modified with phenyl acetate groups have charge selectivity properties and a fast response to changes in analyte concentration. Macro and microelectrodes have been prepared which showed excellent discrimination for cationic dopamine over anionic ascorbic acid [53]. Well-defined differential pulse voltammograms were obtained for oxidation of dopamine in the presence of a 100-fold excess of ascorbic acid at the phenyl acetate modified microelectrodes.

The diazonium coupling method has been used to prepare GC surfaces which are resistant to fouling by protein [54]. Downard and Roddick reported that hydrophilic groups attached to the surface reduced bovine serum albumin (BSA) adsorption. Voltammetry of hydroxymethyl ferrocene was used as a probe of surface fouling. Modification of GC electrodes with phenyl acetate showed little impact on the voltammetry of the probe molecule but significantly reduced the

impact of BSA adsorption. After examining the effects of a range of surface modification, the authors concluded that hydrophilic groups that extend a sufficient distance from the electrode reduce protein adsorption while surface hydrophobicity promoted protein adsorption. The modified electrode could be used for analysis of clinical samples with reduced electrode fouling.

Amperometric detection is commonly utilized with flow analytical techniques such as flow injection analysis, ion chromatography and high performance liquid chromatography. Diazonium reduction method has been utilized to prepare amperometric flow detectors with selectivity based on hydrophobicity and charge [55]. At p-alkyl phenyl modified electrodes, the sensitivity ratio for chlorpromazine: uric acid obtained from amperometric measurements was significantly enhanced over that observed at the polished electrode. At phenylacetate modified electrodes the sensitivity ratios for acetaminophen: uric acid and acetaminophen: ascorbic acid were enhanced over the polished electrode values. These results were explained by considering the impact of the hydrophobicity and charge of the monolayer and analyte.

McCreery's group used the diazonium reduction method for the fabrication of carbon-based molecular junctions, which represented a new paradigm for molecular electronics [56, 57]. A thin layer of oriented organic molecules was positioned between PPF and mercury (Hg). The molecular layer became a component in an electronic circuit and showed properties that strongly depended on molecular structure. The current/voltage behaviour of methyl phenyl, n-butyl phenyl, tert-butyl phenyl and stilbene monolayers between PPF and Hg indicated

a negligible pinhole density and showed weak dependence on temperature. The action of a nitroazobenzene (NAB) molecular junction as a bistable switch was also demonstrated.

Carbon/nitroazobenzene/titanium molecular electronic junctions were characterized with XPS and Raman spectroscopy [57]. NAB was chemisorbed to a PPF substrate by diazonium reduction and a top contact of vapour-deposited titanium (Ti) was used to construct the molecular junctions. The results indicated a reaction between condensing Ti atoms and the terminal NO₂ group, probably forming a Ti-nitroso linkage. This resulted a molecular junction with covalent bonding at both ends. The reaction between Ti and the nitro group appeared to prevent short circuits resulting from the incursion of Ti into the NAB layer.

In most of the work utilizing diazonium reduction method, aryl films have been deposited from acetonitrile solution [40-46, 48, 50, 53-57]. Aqueous acidic solutions have been used as a deposition medium only in a few reports. Dequaire and coworkers used aqueous acidic conditions to attach aryl derivatives to screen printed graphite electrodes for the construction of electrochemical biosensors [52, 58]. Grafting of aryl groups on GC, carbon fiber, iron and mild steel surfaces from acidic medium were reported by Pinson and coworkers [49, 59]. In a recent study, Brooksby and Downard characterized aryl films formed from acidic solutions on PPF surface using electrochemistry and atomic force microscopy [60]. A detailed investigation of diazonium reduction in aqueous media is carried out in this thesis.

Electron Transfer Blocking Studies

The electron transfer (ET) kinetics of solution based redox systems at covalently modified carbon surfaces has been examined with the goal of relating surface structure with reactivity. The effect of electrode modification on redox probe response can provide information about the barrier properties of the monolayer, the effective width over which electron transfer must occur, the monolayer charge and its hydrophobicity /hydrophilicity [47]. The electrochemical response of solution species is also of interest for developing sensors with high sensitivity and selectivity for target analytes.

Cyclic voltammetry is widely used to measure standard rate constants for electron transfer from the separation of cathodic and anodic peak potential (ΔE_p) and scan rate (ν) by the method of Nicholson [61]. The method provides an extremely rapid and simple way to evaluate electrode kinetics. The standard heterogeneous rate constant k° is related to the dimensionless rate parameter ψ by the following equation [61],

$$\psi = \frac{(D_o/D_R)^{\alpha/2} k^\circ}{[\pi D_o \nu (nF/RT)]^{1/2}} \quad (1.1)$$

here D_o and D_R are the diffusion coefficient for oxidized and reduced species, α is the transfer coefficient and ν is the scan rate. For $0.3 < \alpha < 0.7$, the ΔE_p values are nearly independent of α and depend only on ψ . The variation of ΔE_p with ψ has been tabulated [61] and is the basis for calculating k° in quasireversible systems by this method. One needs to measure ΔE_p as a function of ν and then determine ψ to finally estimate k° .

Studies of electron transfer kinetics at modified carbon electrodes have been carried out by several groups. Some of these works will be reviewed in the current section. Chen and McCreery proposed a procedure for classifying redox systems by their kinetics on modified carbon surfaces [62]. GC electrodes were modified to yield surfaces with low oxide content and monolayers of several different adsorbates were also formed on GC. The various GC surfaces were then probed for their electron transfer reactivity with nine redox systems. Several systems, including $\text{Ru}(\text{NH}_3)_6^{2+/3+}$ were insensitive to surface modification and were considered outer sphere. $\text{Fe}_{\text{aq}}^{3+/2+}$, $\text{V}_{\text{aq}}^{3+/2+}$ and $\text{Eu}_{\text{aq}}^{3+/2+}$ are catalyzed by surface carbonyl groups. Ascorbic acid, $\text{Fe}(\text{CN})_6^{3-/4-}$ constituted a third group which were not catalyzed by oxides but required a specific surface interaction.

A quantitative examination of electron transfer across hydrophobic, insulating layers of varying thicknesses has been reported by Yang and McCreery [63]. They examined five organic redox systems, methyl viologen and four phenothiazine derivatives. The reduction of methyl viologen was insensitive to surface modification and k^0 decreased by only 50% when a chemisorbed layer was present. Adsorption is a feature of the voltammetry of phenothiazines at polished GC in aqueous solution and is reduced by a significant but variable amount at 4-nitrophenyl modified electrodes. However, k^0 for all species at 4-nitrophenyl modified electrodes were 50-60% of those at polished GC indicating that adsorption was not required for rapid electron transfer and all species behaved as outer-sphere redox systems. For chlorpromazine, k^0 was studied as a function of monolayer thickness. Tunnelling parameter β , for this system was

determined to be 0.2 \AA^{-1} , consistent with values of $0.14\text{-}0.57 \text{ \AA}^{-1}$ which have been estimated for through-bond tunnelling in conjugated, unsaturated monolayers on metal electrodes.

The blocking effect of 4-carboxyphenyl and 4-nitrophenyl modified GC electrodes has been investigated by Saby *et. al.* [42]. The modified electrodes were characterized by cyclic voltammetry, electrochemical impedance spectroscopy and XPS. The barrier properties of the film depended mainly on electrostatic and electrolyte/solvent effects. Cyclic voltammetry experiments were carried out in aqueous and nonaqueous media with four electroactive probes. In acetonitrile, both types of film completely blocked the electrochemical response of ferrocene and $\text{Fe}(\text{CN})_6^{3-}$. In aqueous media the 4-carboxyphenyl layer is expected to be neutral at low pH and to have an increasing negative charge with increasing pH. The responses of $\text{Fe}(\text{CN})_6^{3-}$ and $\text{Ru}(\text{NH}_3)_6^{3+}$ reflected these changes in surface charge and hydrophobicity. The substituted phenyl layer was much more compact and less permeable in contact with a nonaqueous solvent presumably because the layer was poorly solvated and acted as a barrier for both ionic [$\text{Fe}(\text{CN})_6^{3-}$] and hydrophobic (ferrocene) redox species. The 4-nitrophenyl layer appeared to be more blocking than 4-carboxyphenyl layer and this might be due to greater film thickness or density for 4-nitrophenyl film than the other one.

Investigation of the blocking behaviour of a reduced 4-nitrophenyl layer in aqueous acid was carried out by the same workers [50]. When the surface of the 4-nitrophenyl modified electrode was reduced, amine (NH_2), hydroxylamine

(NHOH) and nitroso (NO) groups were produced. The protonation of these functional groups at low pH, allowed the permeation of $\text{Fe}(\text{CN})_6^{3-}$ through the layer and the electrochemical reaction of the redox probe. The redox reaction of $\text{Ru}(\text{NH}_3)_6^{3+}$ on the other hand, was blocked at the reduced film due to the protonation of the functional groups. The barrier properties changed very significantly even though reduction of nitro groups was incomplete. This points to an important fact that electrode response is dominated by electron transfer at sites which exhibit fastest kinetics, which in this case correspond to the reduced sites of the nitro group.

The barrier properties of 4-phenyl acetate modified electrodes have been examined at pH 7.4 by Downard and coworkers [53]. The layer bears a negative charge at this pH. The voltammetric behaviours of the catechol derivatives dopamine (cationic), 4-methyl catechol (neutral) and 3,4-dihydroxyphenyl acetate (DOPAC, anionic) were compared at polished and modified GC electrodes. Phenylacetate modification increased the apparent rate of electron transfer for dopamine, decreased the rate for DOPAC and had no effect for 4-methylcatechol. Changes in peak potential and current for ascorbic acid and uric acid also indicated a retardation of kinetics for these anionic species. Hence electrostatic interactions between the modifying layer and the solution species appear to influence electrode kinetics.

Biphenyl and nitrobiphenyl modified GC surfaces were examined as voltammetric electrodes for ferrocene, benzoquinone and tetracyanoquinodimethane electrochemistry in acetonitrile [64]. The modified electrodes exhibited

slower electron transfer than unmodified GC, by factors that varied with monolayer and redox system. However, after a negative potential excursion to -2.0 V versus Ag^+/Ag , the modified electrodes exhibited much faster electron transfer kinetics, approaching those observed on unmodified GC. The increased rate of electron tunnelling is attributed to an apparently irreversible structural change in the biphenyl or nitrobiphenyl monolayer. The transition to the "ON" state is associated with electron injection into the monolayer from the GC surface. This results in a reduced HOMO-LUMO gap and a higher electronic conductance.

Research Objective

The electrochemical reduction of aryl diazonium salts at carbon electrodes leads to grafting of aryl groups to the surface. Acetonitrile solution containing tetrabutylammonium tetrafluoroborate as supporting electrolyte is commonly used as the modification medium for deposition of these aryl films. A few reports have demonstrated that aryl films can be deposited from aqueous acidic solutions. The goal of our research was to thoroughly investigate the formation of aryl films from aqueous media. Initially we carried out electrochemical studies on films deposited from acidic solutions and compared the blocking ability of these films to those deposited from acetonitrile solutions. We used polished GC and carbon film electrodes (pyrolyzed photoresist film) for this study. Later we extended our studies to other aqueous solutions having neutral and basic pH, as

deposition medium. Aryl diazonium salts in different supporting electrolytes were characterized by UV-VIS spectroscopic studies.

The aryl films deposited from aqueous and organic media were characterized with Atomic Force Microscopy (AFM) to obtain topographical and spatial information. Carbon film electrodes prepared by electron beam evaporation were used in AFM studies due to their atomic scale flatness and good electrochemical activity. The thicknesses of aryl films were measured by using ECF electrodes patterned by photolithography. In our view, the patterned electrodes provided a more reliable platform for thickness measurement than unpatterned electrodes.

References:

1. Kinoshita, K. In *Carbon: Electrochemical and Physiochemical Properties*, Wiley: New York, 1988.
2. McCreery, R. L. In *Electroanalytical Chemistry*, Vol 17 (A.J. Bard. Ed), Dekker: New York, 1991; Vol 17, pp. 221-374.
3. McCreery, R. L. In *Laboratory Techniques in Electroanalytical Chemistry*, 2nd ed.; Kissinger, P.T., Heineman, W.R., Eds; Dekker: New York, 1996; Chapter 10.
4. McCreery, R. L. In *Interfacial Electrochemistry*, Wieckowski, A., Ed.; Dekker: New York, 1999; Chapter 35.
5. McCreery, R. L.; Cline, K. K.; McDermott, C. A.; McDermott, M. T. *Colloids Surf.* **1994**, *93*, 211.

6. Jenkins, G. M.; Kawamura, K. *Polymeric Carbons – Carbon Fibre, Glass and Char*, Cambridge University Press, Cambridge, England, 1976.
7. Kim, Y. -T.; Scamulis, D. M.; Ewing, A. G. *Anal. Chem.* **1986**, *58*, 1782.
8. Beilby, A. L.; Carlsson, A. *J. Electroanal. Chem.* **1988**, *248*, 283.
9. McFadden, C. F.; Russell, L. L.; Melaragno, P. R.; Davis, J. A. *Anal. Chem.* **1992**, *64*, 1520.
10. Saraceno, R. A.; Engstorm, C. E.; Rose, M.; Ewing, A. G. *Anal. Chem.* **1989**, *61*, 560.
11. Wehmeyer, K. R.; Deakin, M. R.; Wightman, R. M. *Anal. Chem.* **1985**, *57*, 1913.
12. Glass, R. S.; Perone, S. P.; Ciarlo, D. R. *Anal. Chem.* **1990**, *62*, 1914.
13. Schlesinger, R.; Bruns, M.; Ache, H. -J. *J. Electrochem. Soc.* **1997**, *144*, 6.
14. Wring, S. A.; Hart, J. P.; Birch, B. J. *Electroanalysis* **1992**, *4*, 299.
15. Wang, J.; Tian, B. *Anal. Chem.* **1992**, *64*, 1706.
16. Sternitzke, K. D.; McCreery, R. L. *Anal. Chem.* **1990**, *62*, 742.
17. Lyons, A. M.; Hale, L. P.; Wilkins, C. W.; *J. Vac. Sci. Technol.* **1985**, *B*, *3*, 447.
18. Kim, J.; Song, X.; Kinoshita, K.; Madou, M.; White, R. *J. Electrochem. Soc.* **1998**, *145*, 2315.
19. Ranganathan, S.; McCreery, R. L.; Majji, S. M.; Madou, M. *J. Electrochem. Soc.* **2000**, *147(1)*, 277.
20. Ranganathan, S.; McCreery, R. L. *Anal. Chem.* **2001**, *73*, 893.
21. Mattson, J. S.; Smith, C. A. *Anal. Chem.* **1975**, *47*, 1122.

22. Blackstock, J. J.; Rostami, A. A.; Nowak, A. M.; McCreery, R. L.; Freeman, M. R.; McDermott, M. T. *Anal. Chem.* **2004**, *76*, 2544.
23. Watkins, B. F.; Behling, J. R.; Kariv, E.; Miller, L. L. *J. Am. Chem. Soc.* **1975**, *97*, 3549.
24. Elliott, C. M.; Murray, R. W. *Anal. Chem.* **1976**, *48*, 1247.
25. Lennox, J. C.; Murray, R. W. *J. Electroanal. Chem.* **1977**, *78*, 395.
26. Koval, C. A.; Anson, F. C. *Anal. Chem.* **1978**, *50*, 223.
27. Collman, J. P.; Denisevich, P.; Konai, Y.; Marrocco, M.; Koval, C.; Anson, F. C. *J. Am. Chem. Soc.* **1980**, *102*, 6027.
28. Evans, J. F.; Kuwana, T. *Anal. Chem.* **1979**, *51*, 358.
29. Barbier, B.; Pinson, J.; Desamot, G.; Sanchez, M. *J. Electrochem. Soc.* **1990**, *137*, 1757.
30. Park, S. -J.; Donnet, J. -B. *J. Colloid Interface Sci.* **1998**, *206*, 29.
31. Adenier, A.; Chehimi, M. M.; Gallardo, I.; Pinson, J.; Vial, N. *Langmuir* **2004**, *20*, 8243.
32. Deinhammer, R. S.; Ho, M.; Anderegg, J. W.; Porter, M. D. *Langmuir* **1994**, *10*, 1306.
33. Downard, A. J.; Mohamed, A. *Electroanalysis* **1999**, *11*, 418.
34. Anne, A.; Blanc, B.; Moiroux, J.; Saveant, J. M. *Langmuir* **1998**, *14*, 2368.
35. Maeda, H.; Yamauchi, Y.; Hosoe, M.; Li, T. -X.; Yamaguchi, E.; Kasamatsu, M.; Ohmori, H. *Chem. Pharm. Bull.* **1994**, *42*, 1870.
36. Maeda, H.; Hosoe, M.; Li, T. -X.; Itami, M.; Yamauchi, Y.; Ohmori, H. *Chem. Pharm. Bull.* **1996**, *44*, 559.

37. Andrieux, C. P.; Gonzalez, F.; Saveant, J. M. *J. Am. Chem. Soc.* **1997**, *119*, 4292.
38. Nowall, W. B.; Wipf, D. O.; Kuhr, W. G. *Anal. Chem.* **1998**, *70*, 2601.
39. Hayes, M. A.; Kuhr, W. G. *Anal. Chem.* **1999**, *71*, 1720.
40. Delamar, M.; Hitmi, R.; Pinson, J.; Saveant, J. M. *J. Am. Chem. Soc.* **1992**, *114*, 5883.
41. Allongue, P.; Delamar, M.; Desbat, B.; Fagebaume, O.; Hitmi, R.; Pinson, J.; Saveant, J. M. *J. Am. Chem. Soc.* **1997**, *119*, 201.
42. Saby, C.; Oritz, B.; Champagne, G.Y.; Belanger, D. *Langmuir* **1997**, *13*, 6805.
43. Liu, Y.-C.; McCreery, R. L. *J. Am. Chem. Soc.* **1995**, *117*, 11254.
44. Kuo, T. -C.; McCreery, R. L. *Anal. Chem.* **1999**, *71*, 1553.
45. Kariuki, J. K.; McDermott, M. T. *Langmuir* **2001**, *17*, 5947.
46. Kariuki, J. K.; McDermott, M. T. *Langmuir* **1999**, *15*, 6534.
47. Downard, A. J. *Electroanalysis* **2000**, *12*, 1085.
48. Liu, Y.-C.; McCreery, R. L. *Anal. Chem.* **1997**, *69*, 2091.
49. Delamar, M.; Desarmot, G.; Fagebaume, O.; Hitmi, R.; Pinson, J.; Saveant, J. M. *Carbon* **1997**, *35*, 801.
50. Oritz, B.; Saby, C.; Champagne, G. Y.; Belanger, D. *J. Electroanal. Chem.* **1998**, *455*, 75.
51. Bourdillon, C.; Delamar, M.; Demaille, C.; Hitmi, R.; Moiroux, J.; Pinson, J. *J. Electroanal. Chem.* **1992**, *336*, 113.

52. Dequaire, M.; Degrand, C.; Limoges, B. *J. Am. Chem. Soc.* **1999**, *121*, 6946.
53. Downard, A. J.; Roddick, A. D.; Bond, A. M. *Anal. Chim. Acta.* **1995**, *317*, 303.
54. Downard, A. J.; Roddick, A. D. *Electroanalysis* **1995**, *7*, 376.
55. Downard, A. J.; Roddick, A. D. *Electroanalysis* **1997**, *9*, 693.
56. Ranganathan, S.; Steidel, I.; Anariba, F.; McCreery, R. L. *Nano Lett.* **2001**, *1*, 491.
57. Nowak, A. M.; McCreery, R. L. *Anal. Chem.* **2004**, *76*, 1089.
58. Ruffien, A.; Dequire, M.; Brossier, P. *Chem. Commun.* **2003**, 912.
59. Adenier, A.; Bernard, M.-C.; Chehimi, M. M.; Cabet-Deliry, E.; Desbat, B.; Fagebaume, O.; Pinson, J.; Podvorica, F. *J. Am. Chem. Soc.* **2001**, *123*, 4541.
60. Brooksby, P. A.; Downard, A. J. *Langmuir* **2004**, *20*, 5038.
61. Nicholson, R. S.; *Anal. Chem.* **1965**, *37*, 1351.
62. Chen, P.; McCreery, R. L. *Anal. Chem.* **1996**, *68*, 3958.
63. Yang, H.-H.; McCreery, R. L. *Anal. Chem.* **1999**, *71*, 4081.
64. Solak, A. O.; Eichorst, L. R.; Clark, W. J.; McCreery, R. L. *Anal. Chem.* **2003**, *75*, 296.

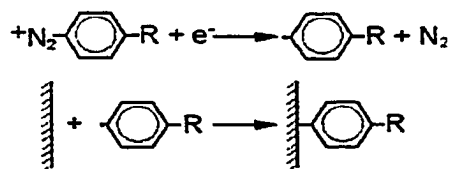
Chapter II

Deposition of Functionalized Aryl Groups on Carbon Electrodes from Aqueous Solutions

Introduction

In this chapter, functionalized aryl groups are deposited on carbon electrodes from aqueous solutions. The blocking properties of the resulting films are examined with electrochemical method.

Modified carbon electrodes have found applications in areas of electron transfer kinetics [1, 2, 3], adhesion promotion in carbon fiber composites [4], control of protein adsorption [5], improvements in electroanalytical selectivity and electrocatalysis [6, 7]. The covalent attachment of aryl groups on carbon surface through electrochemical reduction of diazonium salts was first reported by Delamar and coworkers [8]. Aryl radicals are produced via one- electron reduction of the diazonium salt, which subsequently binds to the surface. The mechanism is shown in Scheme 1.



Scheme 1

The versatility of this method lies in the fact that a large variety of functionalized aryl groups can be grafted easily. The resulting films are strongly bound and require mechanical abrasion to be removed [9]. The phenyl films have

been characterized with electrochemical [1, 6, 8-11], vibrational spectroscopy [2, 12], X-ray photoelectron spectroscopy [1, 9, 12] and scanning probe microscopy [2, 11, 13,14] methods. The reduction method has been used to modify a variety of carbon surfaces, which include glassy carbon (GC) [8, 9], highly oriented pyrolytic graphite (HOPG) [10], screen printed carbon films [15], carbon fibers [4, 16] and pyrolyzed photoresist films (PPF) [9, 13].

In general, these aryl films have been deposited from acetonitrile solution using tetrabutylammonium tetrafluoroborate ($\text{Bu}_4\text{N}^+\text{BF}_4^-$) as the electrolyte [1, 4, 5, 8-11, 17-22]. A few reports have suggested aqueous acidic solutions can be used to graft aryl groups to carbon [4, 15, 23, 24] and one recent study has characterized such films [14]. In this chapter a more thorough investigation of diazonium reduction in aqueous media is undertaken. Aqueous solutions with a range of pH have been investigated. Two types of carbon electrodes were used in this study; polished glassy carbon (GC) and thin carbon film electrodes (pyrolyzed photoresist films). It was reported earlier that the grafting becomes inefficient at $\text{pH} \geq 2$, as the stability of the diazonium decreases [4]. We have used electrochemical measurements to characterize films deposited from different aqueous mediums and also from acetonitrile. UV-VIS spectroscopic studies were carried out to characterize diazonium solutions in different supporting electrolytes. Our findings show that aryl groups form blocking films even when deposited from neutral solutions. These films are comparable to those obtained from acetonitrile in terms of electron transfer blocking ability to solution bound redox species.

Experimental Section

Reagents. 4-Nitrobenzene diazonium tetrafluoroborate (NB) was purchased from Sigma. 4-Phenylacetic acid (PAA) and 4- Biphenyl diazonium tetrafluoroborate (BPDS) were synthesized from the corresponding amino precursors [4-Aminophenyl acetic acid (Acros Organics) and 4- Aminobiphenyl (Aldrich)] according to published procedures [17, 22]. Sulfuric acid (H_2SO_4), potassium chloride (KCl) and sodium hydroxide (NaOH) were obtained from EM Science. Some other reagents used were tetrabutylammonium tetrafluoroborate (Bu_4NBF_4 , Aldrich), acetonitrile (CH_3CN , Caledon) and sodium perchlorate (NaClO_4 , Fisher). Phosphate buffered saline (PBS) having pH values in the range 7-11 were prepared using sodium phosphate monobasic (NaH_2PO_4 , Fisher) or potassium phosphate monobasic (KH_2PO_4 , Caledon). The redox systems studied were as follows: 1 mM dopamine(Sigma) in 0.1M H_2SO_4 , 1 mM $\text{Fe}(\text{CN})_6^{3-}$ (aq) in 1 M KCl from $\text{K}_3\text{Fe}(\text{CN})_6$ (Caledon), 1 mM $\text{Ru}(\text{NH}_3)_6^{3+}$ (aq) in 1 M KCl from $\text{Ru}(\text{NH}_3)_6\text{Cl}_3$ (Stern Chemicals) and 5 mM Eu^{3+} (aq) in 0.2 M NaClO_4 prepared from $\text{Eu}(\text{NO}_3)_3 \cdot 5\text{H}_2\text{O}$ (Aldrich). All reagents were used as received. Aqueous solutions were prepared using Barnstead Nanopure water (18 M Ω -cm). All solutions were purged with argon for 20 minutes before use in electrochemical experiments.

Preparation of Carbon Films. Pyrolyzed photoresist films (PPF) were prepared following the methods described previously [16, 22]. Silicon wafers were diced into 1.2 X 1.2 cm pieces. The pieces were immersed into a 10:1 buffered oxide etch solution (10 parts 40% NH_4F and 1 part 49% HF) to remove

the oxide layer from the surface. Then they were rinsed with water and dried with N₂. A positive photoresist (HPR 504, Arch Chemicals) was spread on each substrate at 200 rpm for 10 s and then spin-coated at 2000 rpm for 40 s. Three coatings were applied on each sample. The photoresist coated samples were placed in a tube furnace filled with forming gas (95% N₂, 5% H₂) for about 30 min. before applying the heating cycle. The samples were heated to a maximum temperature of 1000 °C under flowing forming gas & kept at that temperature for 1.5 hours before cooling down to room temperature in the same forming gas atmosphere. The PPF electrodes were rinsed with Nanopure water and dried with argon before their use in electrochemical measurements.

Electrode Preparation and Electrochemical Measurements. Commercial glassy carbon (Tokai GC-20, Electrosynthesis Corp, NY) electrodes were used in this work. Before starting electrochemical experiments, all GC electrodes were polished successively in 1, 0.3 and 0.05 μm alumina slurries prepared from Buehler alumina powder in nanopure water (18 MΩ-cm) on Buehler polishing microcloth. The electrodes were sonicated in deionized water for 5 minutes between polishing steps.

Electrochemical measurements were performed with a Model AFCBP1 Bipotentiostat (Pine Instruments Company, Grove city, PA) and data was recorded with PineChem (version 2.7.9) software. A standard three- electrode cell was used with a home-made Ag/AgCl/KCl (sat.) as reference electrode and a platinum wire as counter electrode. The electrode area of the working electrode was defined by an elastomeric Viton o-ring (geometric area= 0.28 cm²).

Functionalized aryl layers were deposited by cyclic voltammetry of the corresponding diazonium salt. Scan rate was 100 mV/s unless mentioned.

UV-VIS Spectra. The UV-VIS spectra of aryl diazonium salts in organic and different aqueous solutions were obtained from a Hewlett Packard 8453 single beam spectrometer.

Results and Discussion

Electrochemical Studies on GC Electrodes

Deposition from 0.1M H₂SO₄. GC electrodes were modified with 4-nitrophenyl (NP) film by using a solution of 2.5 mM 4-nitrobenzene diazonium tetrafluoroborate (NB) in 0.1 M H₂SO₄ and applying a potential cycle from 0.45 to -0.10 V vs. Ag/AgCl. Figure 2.1 shows the resulting cyclic voltammogram. An irreversible cathodic wave is observed at 0.166 V in the first cycle, which corresponds to the reduction of NB to a NP radical. This wave disappears in the second cycle and very small current is observed due to the formation of the NP layer during the first cycle. This implies that the formation of the NP layer is almost complete after one cycle.

Electrochemistry of Redox Systems at Modified GC Electrode. The dependence of electrochemical behaviour of carbon electrodes on surface chemistry has been studied extensively [26, 27]. But there lies some difficulties, which include the fact that the carbon surface varies greatly with origin and pretreatment [3]. Thus the surface structure is often unknown. The electron transfer blocking ability of NP film deposited from aqueous acid medium (NP_{AO})

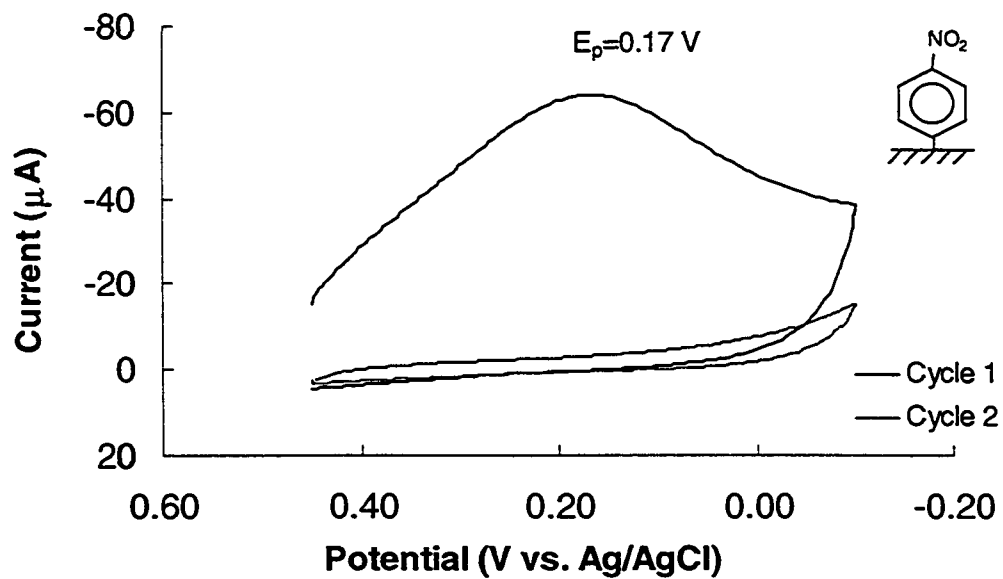


Figure 2.1: Cyclic voltammograms for the reduction of 2.5 mM NB from 0.1 M H_2SO_4 on GC. Scan rate: 100 mV/s.

on GC electrode was examined with three different redox systems. These were $\text{Fe}(\text{CN})_6^{3-/4-}$, $\text{Ru}(\text{NH}_3)_6^{3+/2+}$ and $\text{Eu}_{\text{aq}}^{3+/2+}$ respectively. These redox systems were chosen as they belong to different kinetic classes, based on their sensitivity to surface modifications [3]. $\text{Fe}(\text{CN})_6^{3-/4-}$ in 1M KCl is a benchmark outer sphere redox system. It is not catalyzed by surface oxides but requires a specific surface interaction. The kinetics of $\text{Ru}(\text{NH}_3)_6^{3+/2+}$ is found to be insensitive to surface modification and electron transfer does not depend on an interaction with a surface site or functional group. $\text{Eu}_{\text{aq}}^{3+/2+}$ is a redox system that is dependent on surface oxides. It has been observed that surface carbonyl groups are necessary for facile electron transfer with $\text{Eu}_{\text{aq}}^{3+/2+}$ at carbon electrodes [28].

Figure 2.2 contains cyclic voltammograms of 1 mM $\text{Fe}(\text{CN})_6^{3-/4-}$ in 1 M KCl. First, cyclic voltammetry was carried out at a polished GC electrode. $\text{Fe}(\text{CN})_6^{3-/4-}$ showed fast electron transfer kinetics on polished GC surface, as reflected by the voltammetric peak separation value (ΔE_p) of 65 mV for a 100 mV/s scan rate. Then the cell was rinsed and filled with 2.5 mM NB in 0.1M H_2SO_4 . One potential cycle was carried out to modify the surface. Next, cyclic voltammetry of $\text{Fe}(\text{CN})_6^{3-}$ was performed on this modified surface and a ΔE_p value of 779 mV was obtained. This indicates a significant decrease in the electron transfer rate as compared to a polished GC surface. ΔE_p continued to increase with increase in the number of deposition cycles but became less significant as compared to that after the first cycle. This also indicates that the blocking ability of the NP layer is maximized after the first cycle.

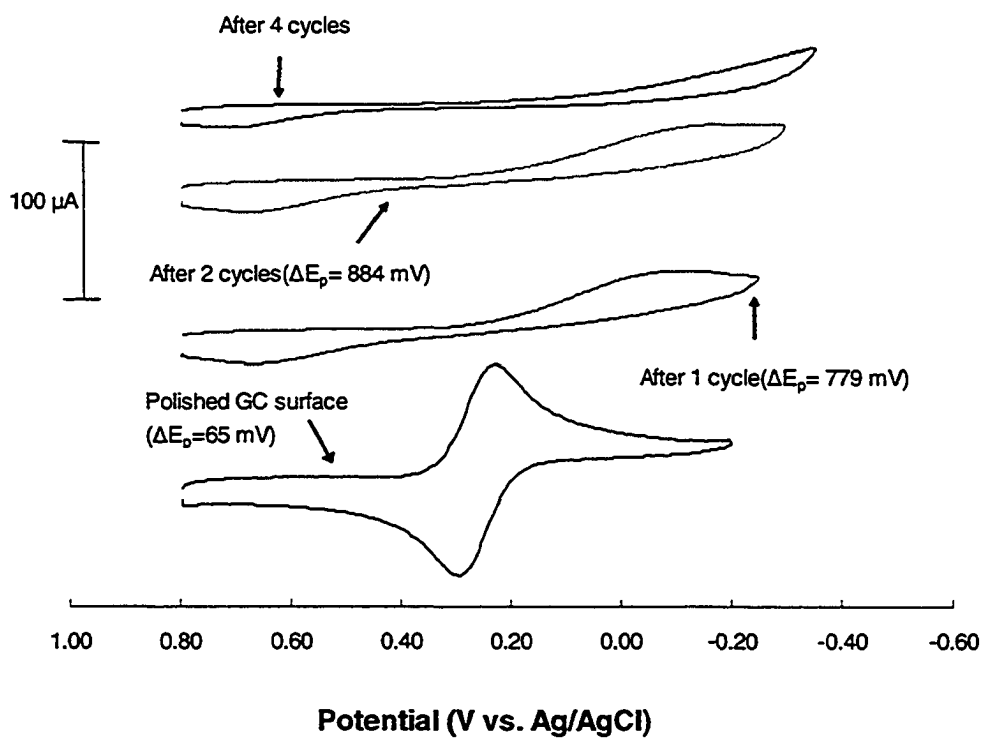


Figure 2.2: Effect of number of deposition cycles of NB (0.1 M H_2SO_4) on blocking of GC surface shown with the voltammetry of 1 mM $\text{Fe}(\text{CN})_6^{3-/4-}$ (1 M KCl).

The study of electron transfer kinetics of $\text{Ru}(\text{NH}_3)_6^{3+/2+}$ redox system was carried out next. Figure 2.3 shows cyclic voltammograms of 1 mM $\text{Ru}(\text{NH}_3)_6^{3+/2+}$ in 1 M KCl. On a polished GC surface, the value of ΔE_p was 72 mV, which indicate fast electron transfer rate. The surface was then modified with one potential cycle of 2.5 mM NB in 0.1 M H_2SO_4 . After that, cyclic voltammetry of $\text{Ru}(\text{NH}_3)_6^{3+}$ was carried out and a ΔE_p value of 115 mV was obtained in this case. This result can be attributed to the increased tunneling distance for electron transfer due to the grafted film. GC surface modified with 2 and 4 potential cycles showed ΔE_p values of 140 and 170 mV respectively. These observations can be attributed to the fact that $\text{Ru}(\text{NH}_3)_6^{3+/2+}$ is a redox system which is relatively insensitive to carbon surface chemistry. There is a small change in ΔE_p for $\text{Ru}(\text{NH}_3)_6^{3+/2+}$, when the surface is coated with a monolayer [3].

Figure 2.4 summarizes the studies done with $\text{Eu}_{\text{aq}}^{3+/2+}$ redox system. The cyclic voltammetry of 5 mM $\text{Eu}(\text{NO}_3)_3^{3+}$ in 0.2 M NaClO_4 , on a polished GC surface, gave a ΔE_p value of 223 mV. Since polished GC surface contains some oxide functionalities hence it shows a reasonable electron transfer rate. After the surface is modified with 1 cycle of NB, the ΔE_p value increases to 820 mV. This reflects a very significant decrease in electron transfer rate as compared to the unmodified GC surface due to the blocking of surface oxides. ΔE_p value obtained for GC surface modified with 2 and 4 potential cycles was 972 mV in both cases. This also indicates that the film formation gets almost complete after the first cycle, which is observed in the case of two other redox species.

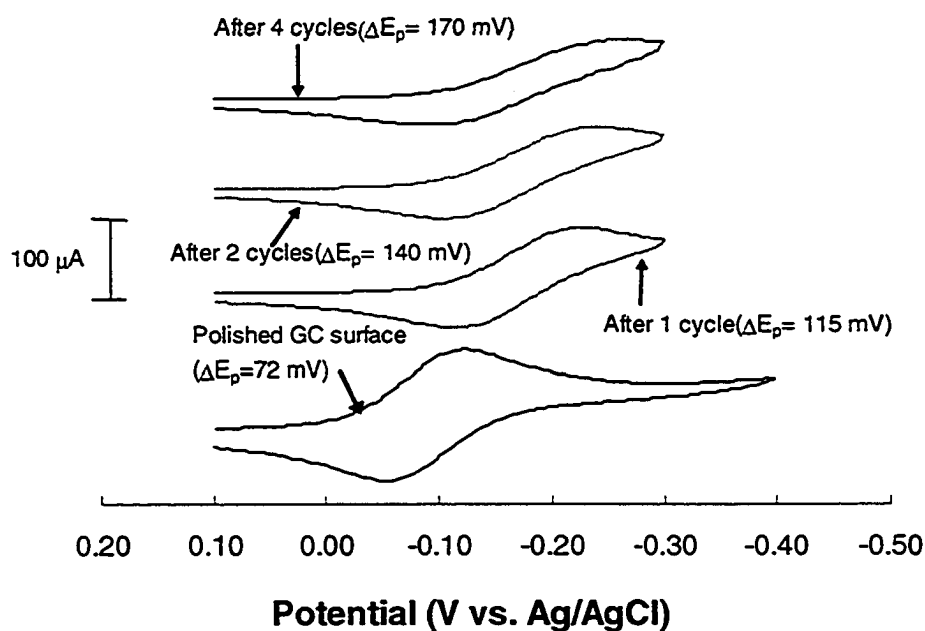


Figure 2.3: Effect of number of deposition cycles of NB (0.1 M H₂SO₄) on blocking of GC surface shown with the voltammetry of 1 mM Ru(NH₃)₆^{3+/2+} (1 M KCl).

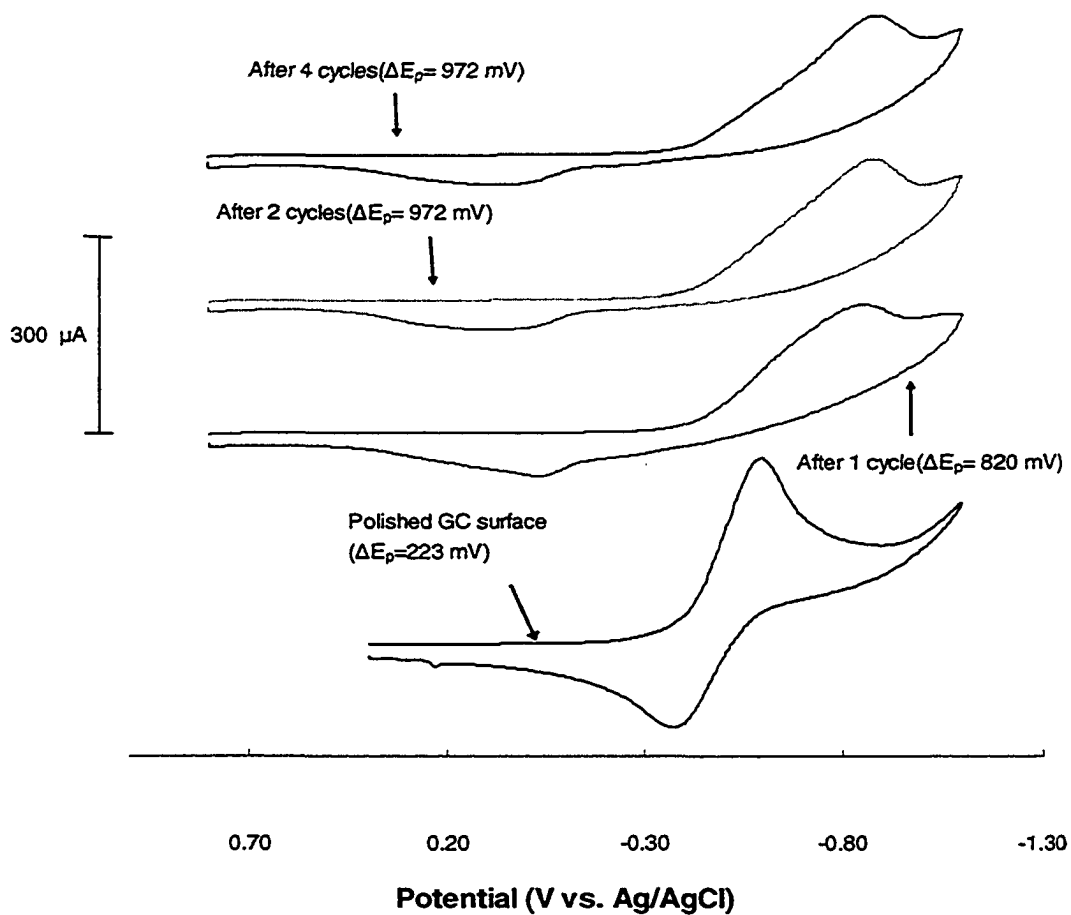


Figure 2.4: Effect of number of deposition cycles of NB (0.1 M H₂SO₄) on blocking of GC surface shown with the voltammetry of 5 mM Eu(NO₃)₃^{3+/2+} (0.2 M NaClO₄).

Deposition from Acetonitrile (CH₃CN). In order to compare the properties of NP film formed by deposition of NB from aqueous acid solution, deposition from organic (CH₃CN) solution was carried out. Acetonitrile is the most common medium used for electrochemical reduction of diazonium salts. Figure 2.5 shows the cyclic voltammogram of 2.5 mM NB in 0.1 M tetrabutylammonium tetrafluoroborate in acetonitrile (0.1M Bu₄NBF₄+ CH₃CN). It presents a chemically irreversible wave ($E_p = 0.161$ V), similar to that observed in aqueous medium. The wave disappears in the second and subsequent cycles and very low current is observed. A small second reduction peak was sometimes observed in the case of deposition from CH₃CN. This is also observed by other workers but its origin has not been fully explored [10, 12, 13].

Electrochemistry of redox systems at modified GC surface. The blocking ability of NP film deposited from CH₃CN (NP_{ACN}) was probed in the presence of electroactive redox species. The results are summarized in Table 2.1, along with those obtained from aqueous deposition. The cyclic voltammetry of Fe(CN)₆³⁻ in 1 M KCl was carried out first at polished GC surface and then at modified surface. The results are summarized in Figure 2.6. On a polished GC surface, the Fe(CN)₆^{3-/4-} couple shows fast electron transfer kinetics ($\Delta E_p = 80$ mV) and this decreases significantly on a surface modified with 1 potential cycle of NB in CH₃CN. A ΔE_p value of 617 mV is obtained in the latter case. As the number of deposition cycle is increased, electron transfer becomes slower (observed with increase in ΔE_p value) but not to a significant extent. This behaviour is similar as observed with films formed by aqueous deposition. The NP film deposited from

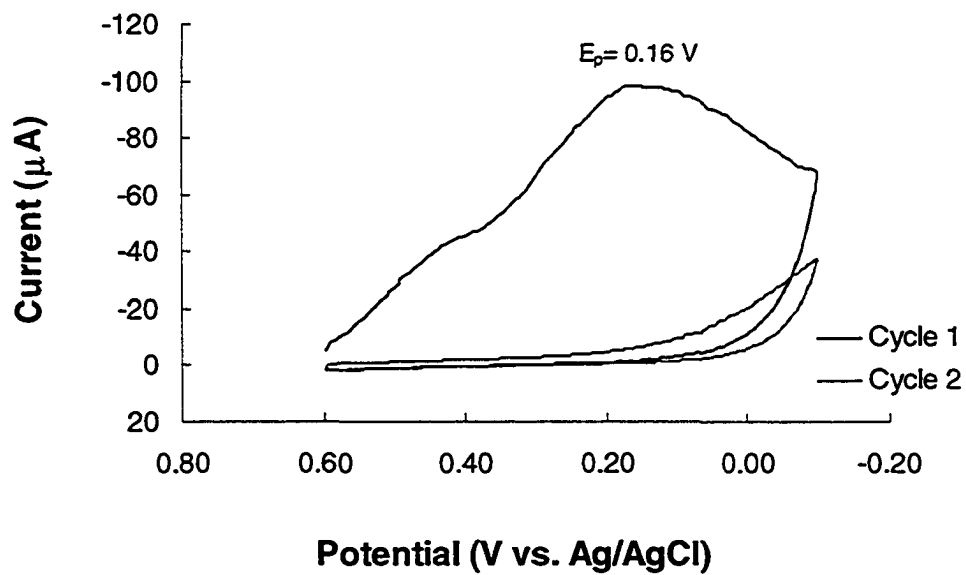


Figure 2.5: Cyclic voltammograms for the reduction of 2.5 mM NB from (0.1 M $\text{Bu}_4\text{NBF}_4 + \text{CH}_3\text{CN}$) on a GC surface. Scan rate: 100 mV/s.

Substrate	Deposition medium	ΔE_p (mV)		
		$\text{Fe}(\text{CN})_6^{3-/4-}$	$\text{Ru}(\text{NH}_3)_6^{3+/2+}$	$\text{Eu}(\text{NO}_3)_3^{3+/2+}$
Polished GC	-	$76^a \pm 10^b$ (N=5) ^c	73 ± 3 (N=7)	228 ± 7 (N=7)
GC modified with 1 deposition cycle	0.1M H_2SO_4	793 ± 20 (N=2)	101 ± 9 (N=5)	820
	0.1M Bu_4NBF_4 + CH_3CN	625 ± 11 (N=2)	108 ± 19 (N=3)	1073 ± 38 (N=4)
GC modified with 2 deposition cycle	0.1M H_2SO_4	882 ± 3 (N=2)	140	972
	0.1M Bu_4NBF_4 + CH_3CN	655	170	1046
GC modified with 4 deposition cycle	0.1M H_2SO_4	> 1100	170	972
	0.1M Bu_4NBF_4 + CH_3CN	676	140	1097

Table 2.1: Results from electrochemical studies on GC electrodes. The surfaces were modified with 2.5 mM NB in aqueous acid (0.1M H_2SO_4) and organic medium (0.1M Bu_4NBF_4 + CH_3CN). Potentials were measured against Ag/AgCl reference electrode and the scan rate was 100 mV/s for all systems.

^a Mean value, ^b Standard deviation, ^c Number of measurements.

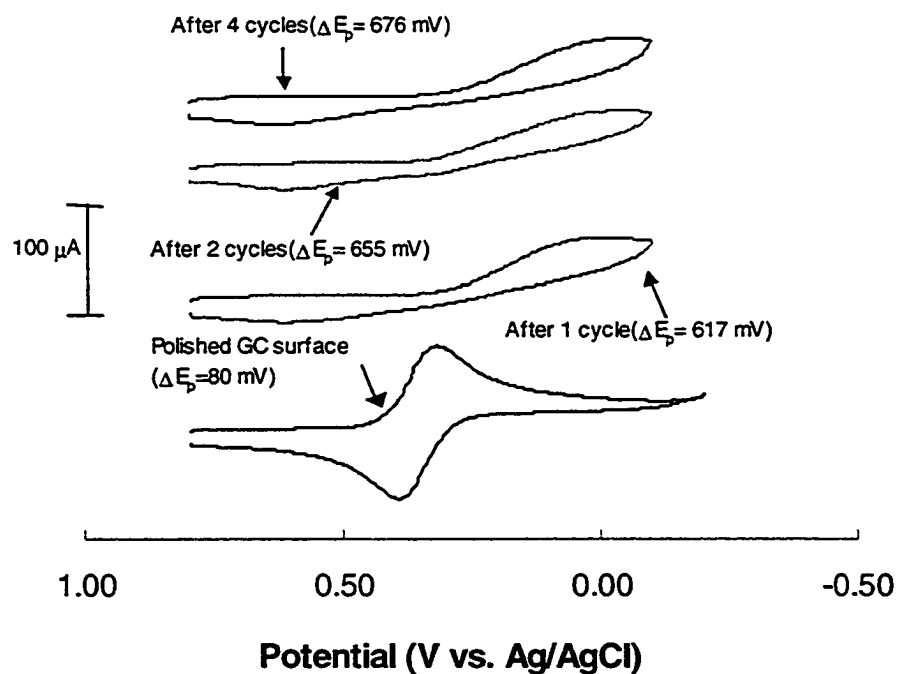


Figure 2.6: Effect of number of deposition cycles of NB (0.1 M $\text{Bu}_4\text{NBF}_4 + \text{CH}_3\text{CN}$) on blocking of GC surface shown with the voltammetry of 1 mM $\text{Fe}(\text{CN})_6^{3-/4-}$ (1 M KCl).

aqueous acid solution appears to be slightly more blocking towards electron transfer of $\text{Fe}(\text{CN})_6^{3-/4-}$, when ΔE_p values are compared in both cases.

The electron transfer kinetics of $\text{Eu}_{\text{aq}}^{3+/2+}$ at GC surface modified with NP film deposited from CH_3CN is shown in Figure 2.7. At polished GC electrode $\text{Eu}_{\text{aq}}^{3+/2+}$ shows a chemically reversible couple ($\Delta E_p = 223$ mV). After 1 deposition cycle, the grafted film blocks the electron transfer significantly as observed from the ΔE_p value of 1027 mV. After 2 and 4 deposition cycles, the values of ΔE_p increase to a small extent. This is also observed in previous cases.

Electrochemical Studies on PPF Electrodes

An examination of aryl film deposition from aqueous and organic solutions on pyrolyzed photoresist film (PPF) surfaces was carried out next. PPF surfaces are very smooth (low surface roughness), which make them an attractive alternative to GC. PPF is also suitable for making patterned electrodes through photolithography.

PPF surfaces were modified with electrochemical reduction of 2.5 mM NB from both aqueous and organic solutions. The modifications were carried out in the same manner as described above and shown in Figure 2.8 and 2.9 respectively. Electron transfer kinetics of three redox systems were carried out on fresh PPF surface and then on surface modified with NP film. The blocking ability of NP film grafted from aqueous and organic solutions are compared using these redox systems. Table 2.2 summarizes the results obtained from these studies.

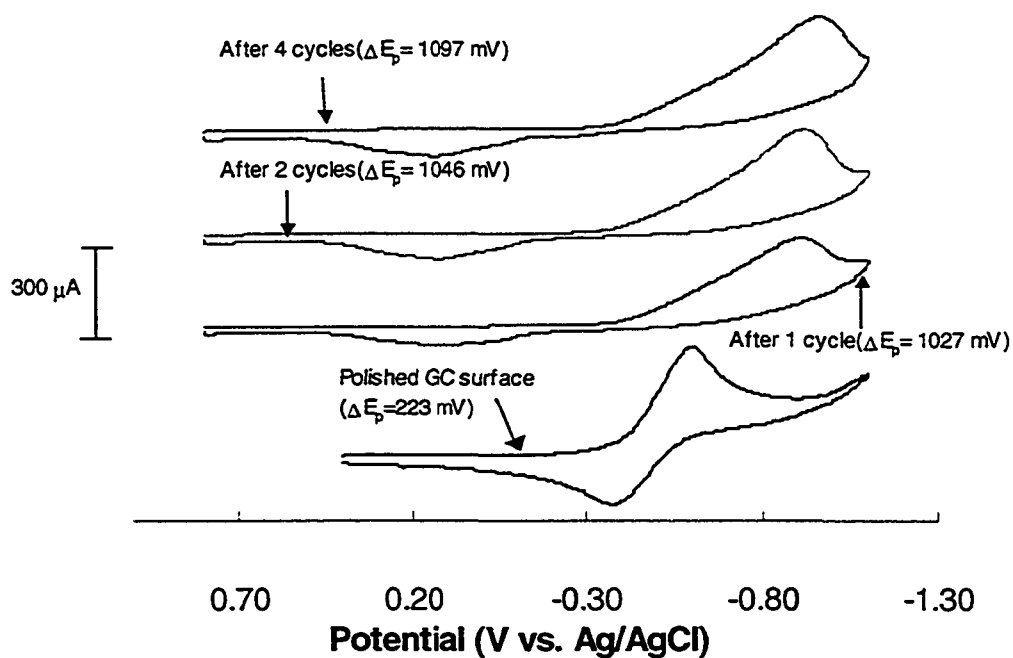


Figure 2.7: Effect of number of deposition cycles of NB (0.1 M $\text{Bu}_4\text{NBF}_4 + \text{CH}_3\text{CN}$) on blocking of GC surface shown with the voltammetry of 5 mM $\text{Eu}(\text{NO}_3)_3^{3+/2+}$ (0.2 M NaClO_4).

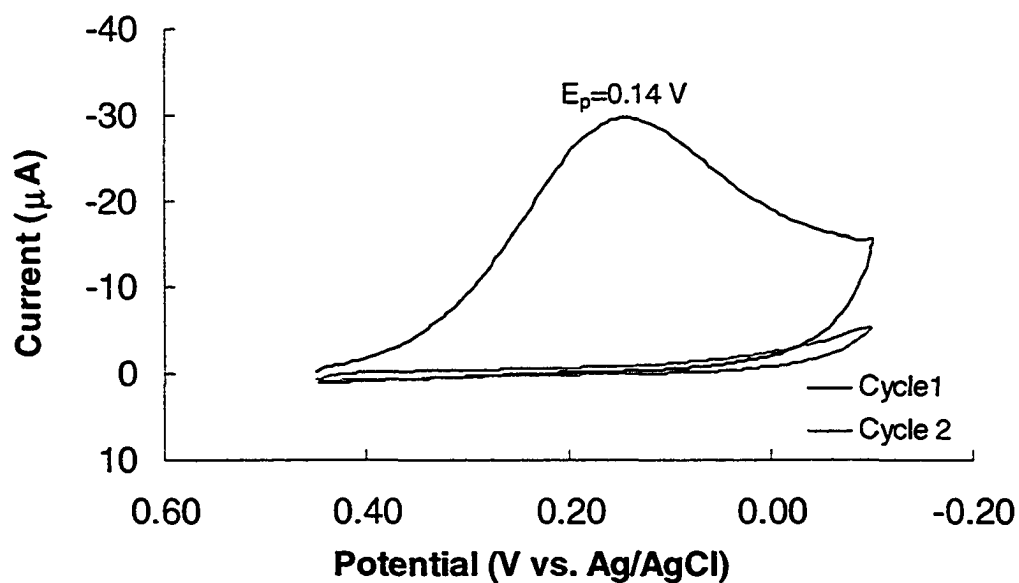


Figure 2.8: Cyclic voltammograms for the reduction of 2.5 mM NB from 0.1 M H_2SO_4 on a PPF surface.

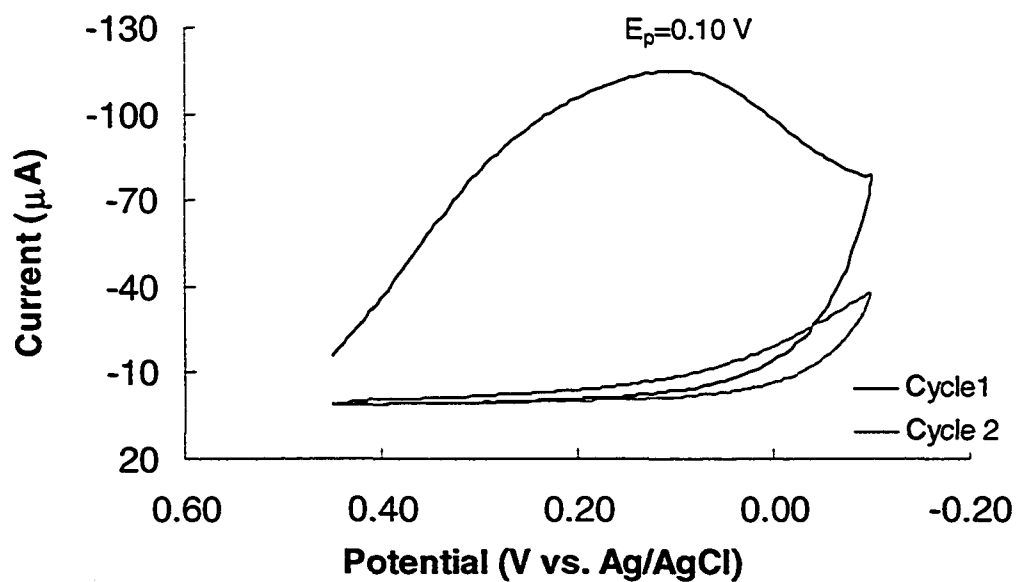


Figure 2.9: Cyclic voltammograms for the reduction of 2.5 mM NB from (0.1 M $\text{Bu}_4\text{NBF}_4 + \text{CH}_3\text{CN}$) on a PPF surface.

Substrate	Deposition medium	ΔE_p (mV)		
		$\text{Fe}(\text{CN})_6^{3-/4-}$	$\text{Ru}(\text{NH}_3)_6^{3+/2+}$	$\text{Eu}(\text{NO}_3)_3^{3+/2+}$
Unmodified PPF	-	144 ± 24 (N=5)	88 ± 8 (N=3)	435 ± 74 (N=2)
PPF modified with 1 deposition cycle	0.1M H_2SO_4	483	224 ± 76 (N=2)	795 ± 8 (N=2)
	0.1M $\text{Bu}_4\text{NBF}_4 + \text{CH}_3\text{CN}$	349 ± 67 (N=2)	170 ± 14 (N=2)	1011
PPF modified with 2 deposition cycle	0.1M H_2SO_4	> 1000	>400	1078
	0.1M $\text{Bu}_4\text{NBF}_4 + \text{CH}_3\text{CN}$	> 1000	273	1141
PPF modified with 4 deposition cycle	0.1M H_2SO_4	> 1000	> 400	1107
	0.1M $\text{Bu}_4\text{NBF}_4 + \text{CH}_3\text{CN}$	> 1000	> 400	1139

Table 2.2: Results from electrochemical studies on pyrolyzed photoresist film (PPF) surface. The surfaces were modified with 2.5 mM NB in aqueous acid (0.1M H_2SO_4) and organic medium (0.1M $\text{Bu}_4\text{NBF}_4 + \text{CH}_3\text{CN}$). Potentials were measured against Ag/AgCl reference electrode and the scan rate was 100 mV/s for all systems.

On a fresh PPF surface, the $\text{Fe}(\text{CN})_6^{3-/4-}$ couple shows reasonable electron transfer rate as indicated by the average voltammetric peak separation value (ΔE_p) of 144 mV. The NP film grafted from 1 potential cycle of 2.5 mM NB in 0.1 M H_2SO_4 appears to block the electron transfer of $\text{Fe}(\text{CN})_6^{3-/4-}$ more efficiently than the film grafted from organic solution. This was also observed by Downard's group [14]. As the number of deposition cycle is increased, films grafted from both media block the electron transfer almost completely. The observation that NP_{AQ} films are more blocking to electron transfer between the electrode and solution bound redox species than the NP_{ACN} films, points to structural difference between the two types of film. This may arise from a range of factors operative during the modification reactions, which include solvation effects, hydrophobic interactions between NP groups and the carbon surface, relative yields for the surface coupling reaction and radical attack on surface-attached NP groups in the two media [14].

The voltammetry of $\text{Ru}(\text{NH}_3)_6^{3+/2+}$ at unmodified PPF showed a ΔE_p value of 88 mV, which indicates relatively fast electron transfer kinetics. Then the surface is modified with 1 potential cycle of NB and electron transfer to the redox species is hindered due to the grafted layer. This is indicated by an increase in ΔE_p value. In this case NP films, grafted from both aqueous and organic solutions exhibited similar blocking properties.

The cyclic voltammetry of $\text{Eu}_{\text{aq}}^{3+/2+}$ in 0.2 M NaClO_4 showed a ΔE_p value of 435 mV on unmodified PPF surface. The electron transfer rate is significantly slower on PPF, when compared to a polished GC surface. This is typical of

$\text{Eu}(\text{NO}_3)_3^{3+/2+}$ on carbon surfaces with a low density of surface oxides [29]. When the PPF surface is modified with 1 potential cycle of NB, the electron transfer rate decreases significantly. Interestingly $\text{Eu}(\text{NO}_3)_3^{3+/2+}$ showed electron transfer kinetics on PPF surface modified with 4 deposition cycles of NB, which was not observed in case of other redox species. This result again confirms the fact that redox systems vary greatly in their sensitivity to surface structure [3].

Investigation of the Effect of pH

The results obtained in the previous sections showed that covalently bound aryl groups can be deposited on the GC and PPF surface from aqueous acid solution (0.1 M H_2SO_4). The phenyl layers that are formed can effectively block electron transfer to solution bound redox species. Therefore we carried out depositions from some other aqueous solutions and investigated the electron transfer blocking ability of the aryl films that are formed. The ultimate goal was to investigate if the pH of the deposition medium had any effect in the formation and blocking ability of the aryl films. Three different aryl diazonium salts with different functional groups were used in this study. These were 4-nitrobenzene diazonium tetrafluoroborate (NB), 4-phenyl acetic acid diazonium tetrafluoroborate (PAA) and 4-biphenyl diazonium tetrafluoroborate (BP).

Deposition of NB. Figure 2.10 summarizes the work done to investigate the effect of pH of the deposition medium in the formation of NP films on GC. Solutions consisted of 2.5 mM NB in either 1 M KCl (pH=4.0), 0.1 M phosphate buffered saline (pH=7.0) or 0.1 M NaOH (pH=12.5). Two potential cycles were

used to deposit NB films. Dopamine (DA) was used to examine the electron transfer blocking ability of the aryl films. Dopamine is a quasi-reversible redox system, which has been used extensively because of its importance to neurochemistry [26]. Dopamine requires an adsorption site for rapid oxidation and is electro-inactive on GC surfaces completely covered by nitrophenyl or trifluoromethyl monolayers [7, 30]. So DA oxidation in water provides a useful test of the presence of pinholes in phenyl layers [22].

In Figure 2.10 cyclic voltammetry of 1 mM DA in 0.1 M H₂SO₄ on polished GC shows reasonably high electron transfer rate with a ΔE_p value of 88 mV. Then GC surface was modified with 2 cycles of NB in CH₃CN (0.1 M Bu₄NBF₄) and DA response was tested on the modified surface. This procedure was repeated for modifying GC surface with NB deposited from 0.1 M H₂SO₄, 1 M KCl, 0.1 M PBS and 0.1 M NaOH solution respectively. The NP film deposited from 0.1 M H₂SO₄ (pH = 1.6), CH₃CN (pH=2.9), 1 M KCl (pH = 4.0) and 0.1 M PBS (pH = 7.0) strongly blocks the electron transfer reaction of DA as shown by the small current obtained under these conditions. However, deposition of NB from 0.1 M NaOH (pH = 12.5) fails to block the surface of GC as shown by the high DA activity ($\Delta E_p = 179$ mV). 2.5 mM NB was deposited on GC from several other phosphate buffer solutions having pH in the range of 8-11 and DA response was examined in each of the modified surface. DA activity could be observed on surfaces modified with NB solution having pH greater than 8. So it can be concluded that NP films blocks the GC surface when NB is deposited from solutions of pH < 8.

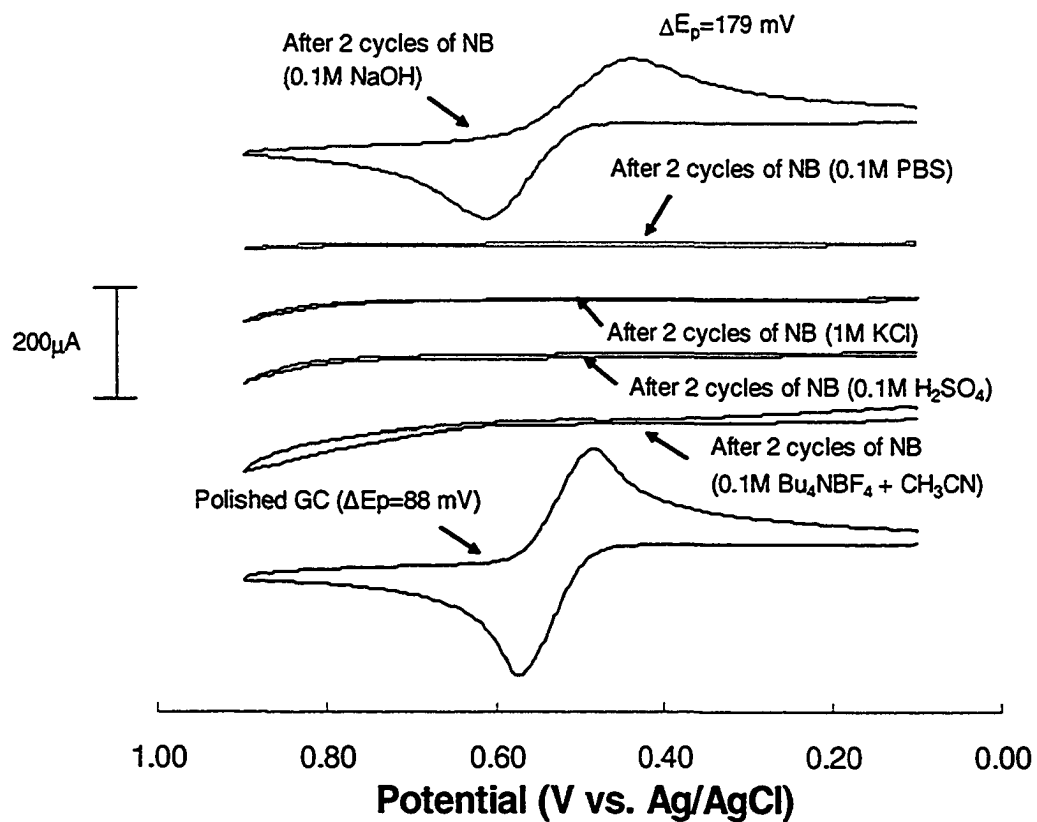


Figure 2.10: Voltammetry of 1 mM DA (0.1 M H₂SO₄) on GC surfaces modified with NB from solutions of various pH.

Deposition of PAA. The effect of pH of the deposition medium in the formation of aryl layers was investigated next using 4-phenyl acetic acid diazonium tetrafluoroborate (PAA). 5mM PAA in a variety of supporting electrolyte were used to modify the GC surface. Usually 2 deposition cycles were carried out. For example, Figure 2.11 shows the voltammetry of 5 mM PAA in (0.1 M $\text{Bu}_4\text{NBF}_4 + \text{CH}_3\text{CN}$) on polished GC. Only in case of PAA in 0.1 M NaOH, 5 deposition cycles were performed. Dopamine voltammetry on the modified surface was used to detect pinholes in the PAA films.

Figure 2.12 shows the ET blocking results obtained in this study. The cyclic voltammetry of 1 mM DA in 0.1 M H_2SO_4 on a polished GC electrode exhibits a ΔE_p value of 101 mV. This is slightly higher than that observed in Figure 2.10 illustrating the variability of polished GC surface. The voltammetry of DA showed very little current on a surface modified from CH_3CN indicating that the PAA film completely covered the GC surface. As shown in Figure 2.12, PAA films formed from aqueous solutions generally do not completely block DA voltammetry. DA exhibits low, but measurable ET rates on films deposited from 0.1 M H_2SO_4 ($\Delta E_p=506$ mV), 0.1M PBS ($\Delta E_p=360$ mV) and 0.1M NaOH ($\Delta E_p=187$ mV). It can be recalled from Figure 2.10 that NB formed layers that completely blocked DA electron transfer, when deposited from solutions with $\text{pH}<8$. The pK_a of PAA is ~ 4.3 . Figure 2.12 shows that similar films are formed in 0.1 M H_2SO_4 ($\text{pH}=1.6$) and 0.1 M PBS ($\text{pH}=6.8$), suggesting that ionization of the acid group does not play a role in film formation. We believe that the higher

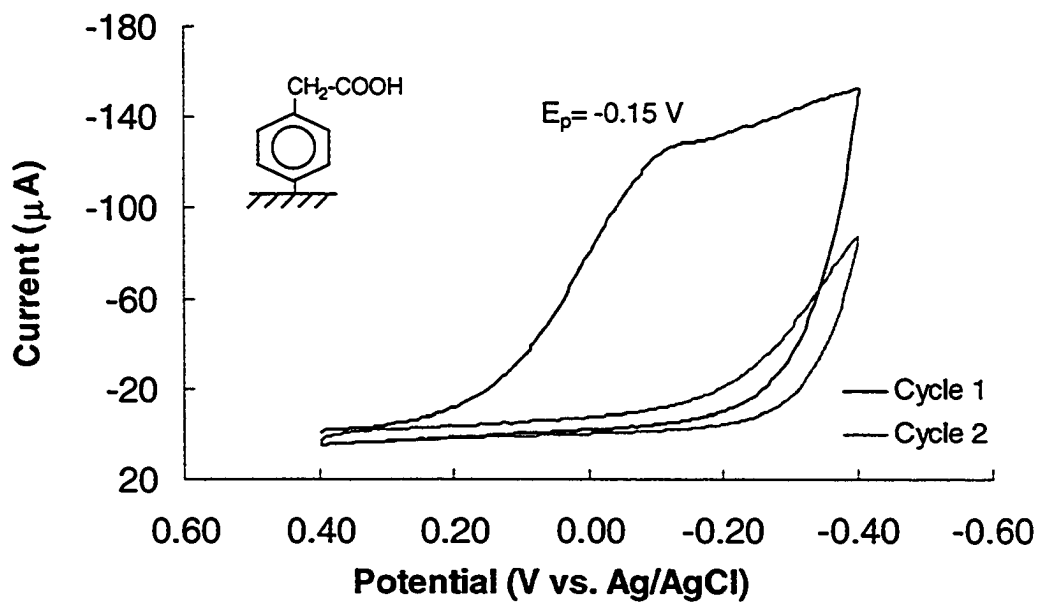


Figure 2.11: Cyclic voltammograms for the reduction of 5 mM PAA from (0.1 M $\text{Bu}_4\text{NBF}_4 + \text{CH}_3\text{CN}$) on a GC surface.

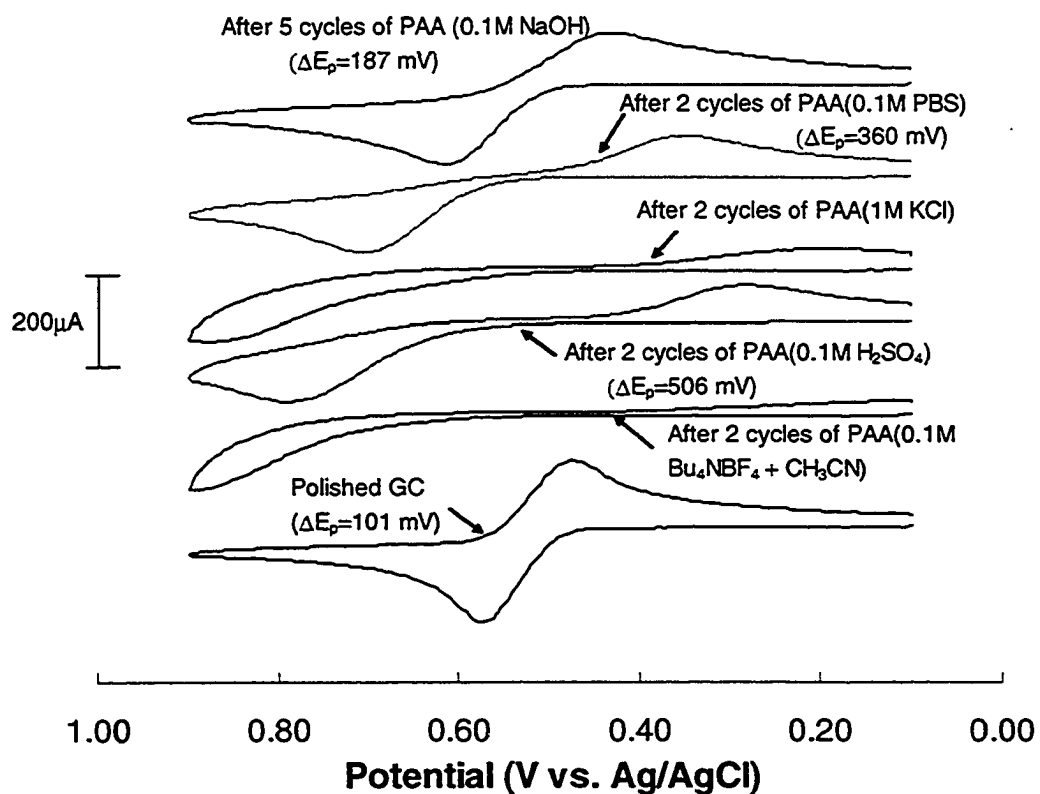


Figure 2.12: Voltammetry of 1 mM DA (0.1 M H_2SO_4) on GC surfaces modified with PAA from solutions of various pH.

solubility of PAA in aqueous solutions may influence film formation. We thus investigated a third diazonium salt.

Deposition of BP. The electrochemical reduction of 4-biphenyl diazonium tetrafluoroborate (BP) in different supporting electrolytes was carried out on GC. Figure 2.13 shows the deposition BP film using two potential cycles of 1mM BP in (0.1M Bu₄NBF₄ + CH₃CN), from +0.7 V to -0.6 V vs. Ag/AgCl. Cyclic voltammetry of 1mM DA in 0.1M H₂SO₄ was then carried out on the modified GC surface to investigate the nature of the BP films. Figure 2.14 summarizes the results obtained in this study. BP films formed in CH₃CN and aqueous solutions with pH up to 7 completely block DA voltammetry. This supports our belief that solubility may play a role in film formation. We observed that PAA dissolves more easily in aqueous solutions than NB and BP. The higher solubility may lead to films that are less dense compared to NB and BP. Molecules with higher solubility experience less driving force to form films on a substrate over a short period of time. In all cases, films formed from 0.1 M NaOH exhibited very little DA blocking. Hence it can be concluded that aryl groups deposited from basic solutions form incomplete films.

UV-VIS Spectra of Aryl Diazonium Salts. The formation of aryl films is dependent on the pH of the deposition medium. To further investigate this pH dependence, we examined the UV-VIS spectra of the aryl diazonium salts in different supporting electrolytes. The results are shown in Figs. 2.15-2.17 and Table 2.3.

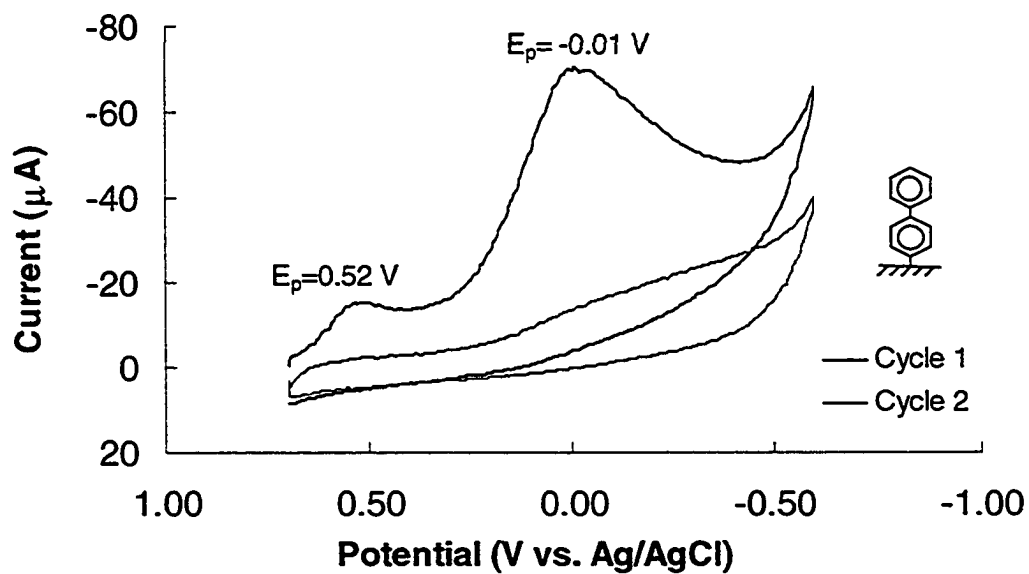


Figure 2.13: Cyclic voltammograms for the reduction of 1 mM BP from (0.1 M $\text{Bu}_4\text{NBF}_4 + \text{CH}_3\text{CN}$) on a GC surface.

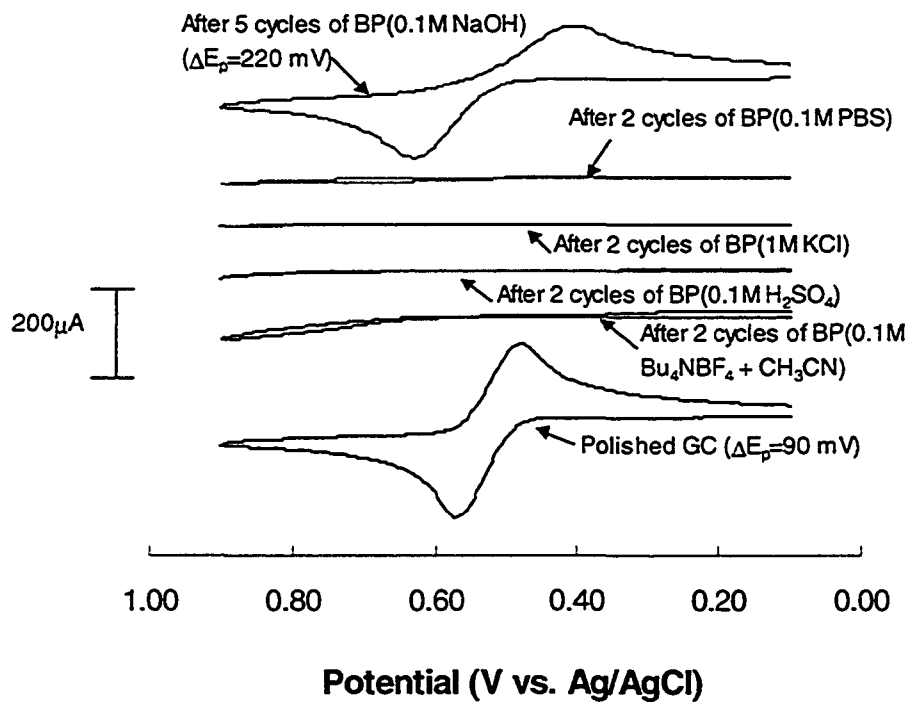


Figure 2.14: Voltammetry of 1 mM DA (0.1 M H₂SO₄) on GC surfaces modified with BP from solutions of various pH.

The electronic spectra of para-substituted benzene diazonium tetrafluoroborates have a single band in the range of 260-380 nm ($\log \epsilon > 4.0$) [31]. This is observed in the spectra in Figure 2.15. The absorbance maxima (A_{\max}) is strongly dependent on substituents and their positions. The spectra of NB in three different supporting electrolytes (0.1M $\text{Bu}_4\text{NBF}_4 + \text{CH}_3\text{CN}$, 0.1M H_2SO_4 and 1M KCl) showed absorption maxima around 260 and 311 nm, consistent with values found in literature [32, 33]. However the spectra of NB in 0.1M NaOH showed maxima at 330 and 218 nm, which indicates that the NB diazonium salt precursor undergoes a chemical transformation at high pH. Similarly the spectra of BP showed maxima at 341 nm in organic, aqueous acid and 1M KCl solution (Figure 2.16). This peak is absent in basic solution. In 0.1M NaOH, BP showed maxima at 218 and 283 nm. The spectra of PAA showed maxima around 274 nm in organic, aqueous acid and 1M KCl solution, whereas in 0.1M NaOH the maxima is at 217 nm (Figure 2.17).

This result can be attributed to the fact that aryl diazonium ions react with alkaline solution and equilibrate to diazohydroxide and diazotate [34].



At high pH the forward reaction of ArN_2^+ and OH^- becomes appreciable [32]. Hence the absorption maxima obtained for diazoniums in 0.1M NaOH are probably due to the diazohydroxide and diazotate species. As a result, aryl diazonium ions are less available for reduction to aryl radicals, which subsequently forms the aryl films. So incomplete films are formed in basic solutions, which is also observed in our ET blocking studies.

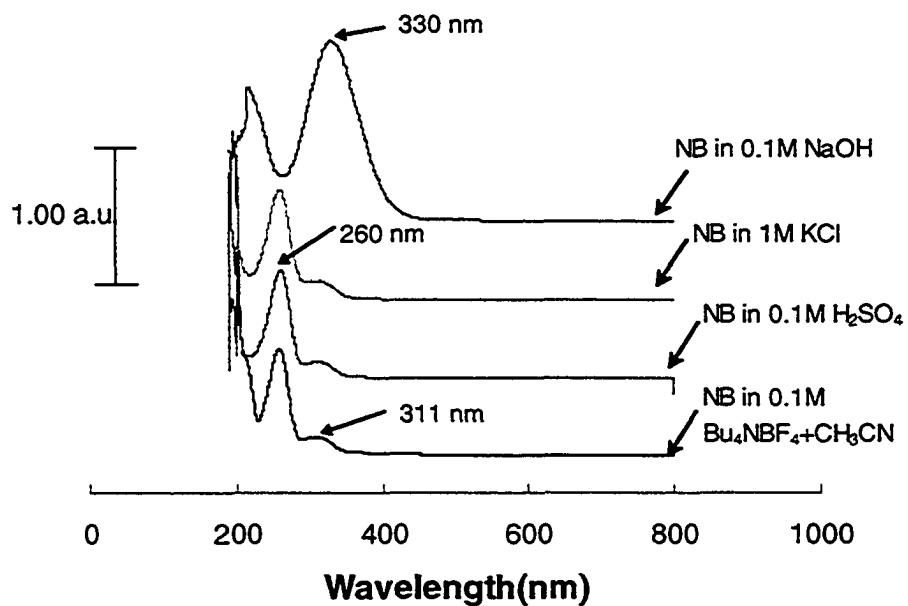


Figure 2.15: UV-VIS spectra of NB in different supporting electrolytes.

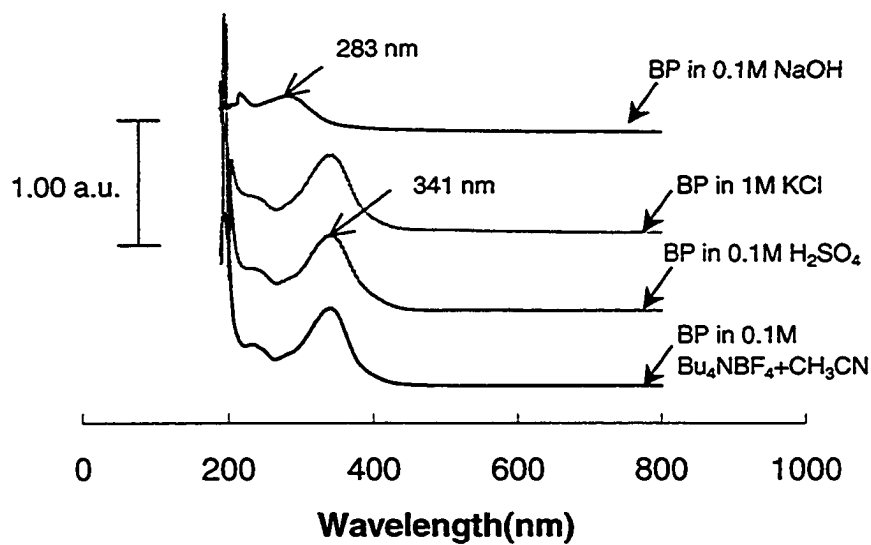


Figure 2.16: UV-VIS spectra of BP in different supporting electrolytes.

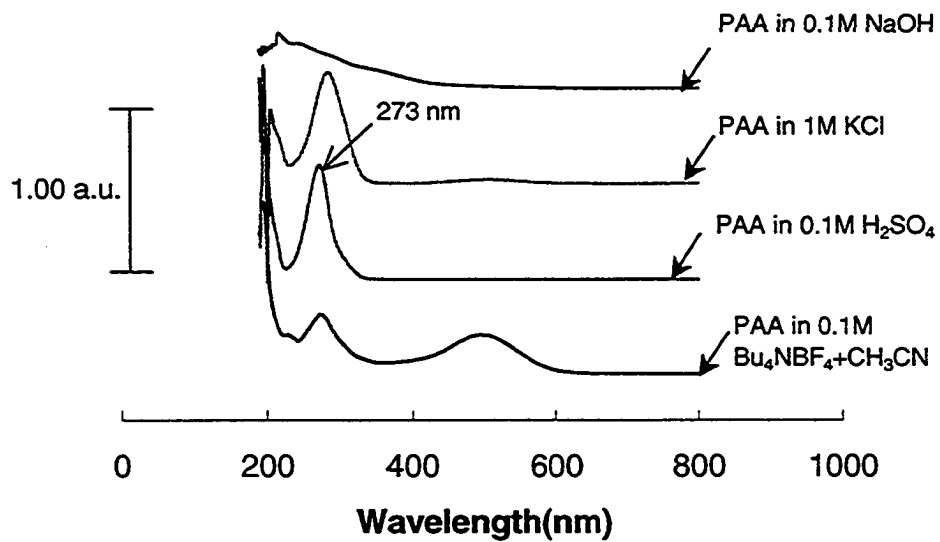


Figure 2.17: UV-VIS spectra of PAA in different supporting electrolytes.

Diazonium compound	A_{\max} (nm)			
	0.1M Bu_4NBF_4 + CH_3CN	0.1M H_2SO_4	0.1M KCl	0.1M NaOH
NB	196		203	
	259	260	260	330
	309	311	312	218
PAA	228	195	206	
	274	273	284	217
	496			
BP	194		205	218
	341	341	341	283
	232	232		

Table 2.3: Results of UV-VIS spectra of diazoniums in different supporting electrolytes.

Conclusions:

Glassy carbon and PPF electrodes were successfully modified with covalently bound NP groups from aqueous acid (0.1M H₂SO₄) solution. The layers that were formed effectively blocked electron transfer to solution bound redox species. The blocking ability of the layer was maximized after the first deposition cycle. When compared with NP films deposited from organic (0.1M Bu₄NBF₄ + CH₃CN) solution, the NP_{AQ} films blocked the electron transfer of Fe(CN)₆^{3-/4-} redox species more efficiently than the NP_{ACN} films. This is indicative of structural difference between the two types of film. The formation of blocking film by aryl groups is strongly dependent on the pH of the deposition medium and occurs at acidic to neutral pH solutions. The results also suggest that aryl groups with higher solubility in aqueous solutions, form less robust films. Electrodes are very poorly blocked by aryl groups deposited from strong basic solution. UV-VIS spectra suggest that the diazonium group reacts chemically in basic solutions and is no longer available to be reduced to the aryl radical.

References

1. Saby, C.; Oritz, B.; Champagne, G.Y.; Belanger, D. *Langmuir* **1997**, *13*, 6805.
2. Kariuki, J. K.; McDermott, M. T. *Langmuir* **2001**, *17*, 5947.
3. Chen, P.; McCreery, R. L. *Anal. Chem.* **1996**, *68*, 3958.
4. Delamar, M.; Desarmot, G.; Fagebaume, O.; Hitmi, R.; Pinson, J.; Saveant, J. M. *Carbon*, **1997**, *35*, 801.

5. Downard, A. J.; Roddick, A. D.; Bond, A. M. *Anal. Chim. Acta.* **1995**, *317*, 303.
6. Downard, A. J. *Langmuir* **2000**, *16*, 9680.
7. Duvall, S.H.; McCreery, R. L. *Anal. Chem.* **1999**, *71*, 4594.
8. Delamar, M.; Hitmi, R.; Pinson, J.; Saveant, J. M. *J. Am. Chem. Soc.* **1992**, *114*, 5883.
9. Allongue, P.; Delamar, M.; Desbat, B.; Fagebaume, O.; Hitmi, R.; Pinson, J.; Saveant, J. M. *J. Am. Chem. Soc.* **1997**, *119*, 201.
10. Liu, Y.-C.; McCreery, R. L. *Anal. Chem.* **1997**, *69*, 2091.
11. Kariuki, J. K.; McDermott, M. T. *Langmuir* **1999**, *15*, 6534.
12. Liu, Y.-C.; McCreery, R. L. *J. Am. Chem. Soc.* **1995**, *117*, 11254.
13. Anariba, F.; Duvall, S. H.; McCreery, R. L. *Anal. Chem.* **2003**, *75*, 3837.
14. Brooksby, P. A.; Downard, A. J. *Langmuir* **2004**, *20*, 5038.
15. Dequaire, M.; Degrand, C.; Limoges, B. *J. Am. Chem. Soc.* **1999**, *121*, 6946.
16. Ranganathan, S.; McCreery, R. L. *Anal. Chem.* **2001**, *73*, 893.
17. Yang, H.-H.; McCreery, R. L. *Anal. Chem.* **1999**, *70*, 4081.
18. Ray, K.; McCreery, R. L. *Anal. Chem.* **1997**, *69*, 4680.
19. Kuo, T. -C.; McCreery, R. L. *Anal. Chem.* **1999**, *71*, 1553.
20. Liu, S.; Tang, Z.; Shig, Z.; Niu, L.; Wang, E.; Dong, S. *Langmuir* **1999**, *15*, 7268.
21. Downard, A. J.; Prince, M. J. *Langmuir* **2001**, *17*, 5581.

22. Solak, A. O.; Eichorst, L. R.; Clark, W. J.; McCreery, R. L. *Anal. Chem.* **2003**, *75*, 296.
23. Adenier, A.; Bernard, M.-C.; Chehimi, M. M.; Cabet-Deliry, E.; Desbat, B.; Fagebaume, O.; Pinson, J.; Podvorica, F. *J. Am. Chem. Soc.* **2001**, *123*, 4541.
24. Ruffien, A.; Dequaire, M and Brossier, P. *Chem. Commun.* **2003**, 912.
25. Ranganathan, S.; McCreery, R. L.; Majji, S. M.; Madou, M. *J. Electrochem. Soc.* **2000**, *147(1)*, 277.
26. McCreery, R. L. In *Electroanalytical Chemistry*, Vol 17 (A.J. Bard. Ed), Dekker: New York, 1991, pp. 221-374.
27. Kinoshita, K. In *Carbon: Electrochemical and Physiochemical Properties*, Wiley: New York, 1988.
28. Chen, P.; Fryling, M. A.; McCreery, R. L. *Anal. Chem.* **1995**, *67*, 3115.
29. McDermott, C. A.; Kneten, K. R.; McCreery, R. L. *J. Electrochem. Soc.* **1993**, *140*, 2593.
30. Duvall, S.H.; McCreery, R. L. *J. Am. Chem. Soc.* **2000**, *122*, 6759.
31. Ben-Efraim, D.A.; In *The Chemistry of Diazonium and Diazo Groups*, Part 1 (Saul Patai, Ed.), John Wiley & Sons, 1978, p.165.
32. Lewis, E. S. and Suhr, H. *J. Am. Chem. Soc.*, **1958**, *80*, 1367.
33. Zollinger, H., In *Azo and Diazo Chemistry*, Interscience: New York, 1961, pp. 64-65.
34. Hegarty, A. F. In *The Chemistry of Diazonium and Diazo Groups*, Part 2 (Saul Patai, Ed.), John Wiley & Sons, 1978, pp. 532-536.

Chapter III

Patterning Method to Evaluate the Thickness of Aryl layers on Carbon Surfaces Deposited from Various Media

Introduction

The electrochemical reduction of diazonium salts has been used to derivatize the surfaces of carbon [1-6], silicon [7, 8] iron [9], cobalt, nickel, copper, zinc, platinum and gold [10]. It was initially proposed that diazonium reduction forms covalently bound monolayers on surface [1], however, multilayer aryl films have been reported by several groups [11-15]. A possible mechanism for multilayer formation involves the attachment of free aryl radicals in solution to a surface bound aryl group [11]. The observation of multilayer formation from depositions in CH₃CN prompted us to investigate the thickness of films deposited from aqueous solutions. Our group has previously used atomic force microscopy (AFM), combined with surface patterning to measure the thickness of aryl films on GC [12]. An AFM based scratching method has also been used to measure film thickness on PPF surface [14-16].

In the current Chapter, ultraflat electron-beam deposited carbon film (ECF) electrodes were patterned using photolithography and then modified with aryl films. These easily prepared thin film electrodes possess good electrochemical activity and near atomic scale flatness [17]. The modified substrates provide a reliable platform for measuring the thickness of aryl films with AFM. The self-assembly of aryl groups on carbon surfaces from diazonium salt solutions was also investigated in this study.

Experimental Section

Reagents. The following reagents were used as received: tetrabutylammonium tetrafluoroborate (Bu_4NBF_4 , Aldrich), acetonitrile (CH_3CN , HPLC grade, Aldrich), sulfuric acid (EM Science), 2-propanol (IPA, Fisher), hydrofluoric acid (HF, Fisher), hydrogen peroxide (H_2O_2 , Merck), xylene (ACP Chemicals). 4-Nitrobenzene diazonium tetrafluoroborate (NB) was purchased from Sigma. 4-Biphenyl diazonium tetrafluoroborate (BP) was synthesized from 4-Aminobiphenyl (Aldrich) according to a published procedure [18]. All solutions were purged with argon for 20 minutes before using in electrochemical experiments. Aqueous solutions were prepared in Nanopure water (Barnstead, 18 M Ω -cm).

Preparation of e-Beam Deposited Carbon Films (ECF). Thin film carbon electrodes were prepared by electron beam evaporation according to a method developed in our lab [17]. 50 nm carbon films were deposited onto highly doped silicon wafers in an electron beam evaporation vacuum chamber. Silicon wafers (N-type, arsenic doped, Silicon Valley Microelectronics) were diced into 1.2 cm \times 1.2 cm sized substrates. The substrates were immersed in piranha solution (1:3 (v/v) 30% H_2O_2 /concentrated H_2SO_4) for 15 minutes and then washed in deionized water. This removes any organic contaminant present in the surface. Next the substrates were dipped in 49% HF for 1 minute to remove oxide layer from the surface. The substrates were washed thoroughly with deionized water and dried with argon. The cleaned samples were loaded directly into the

evaporation chamber. High-purity polycrystalline graphite was used as the source for evaporation of carbon.

Pattern Formation on ECF Electrodes. ECF electrodes were patterned by using standard photolithographic technique. Photolithography is the process of transferring patterns onto a substrate by optical means. First, a photosensitive film (photoresist) is coated on the substrate to uniform thickness, by spin coating. Then the substrate is soft baked to evaporate the coating solvent and to densify the photoresist. A mask is used, which contains the desired pattern to be transferred on the resist-coated substrate. A photo mask, which is widely used, is a nearly optically flat glass or quartz plate with an absorber pattern metal (a chromium layer). The photo mask is set in a mask-aligner/exposure tool. It is aligned to the photoresist coated wafer and exposed by UV radiation. The absorber pattern on the photo mask is opaque to UV light, whereas glass and quartz are transparent. Exposure changes photoresist solubility, which enables selective removal of resist in the development step. In positive photoresists, the exposed areas become more soluble in the developer solution. Conversely, in the negative photoresist, the exposed parts become insoluble in the developer. In both cases, the remaining photoresist acts as a protective mask for subsequent modification steps.

In our work, first the surface of the ECF electrodes were cleaned by sonicating in a 50:50 2-propanol / acetonitrile (v/v) mixture for 10 minutes. One coat of a negative photoresist (IC 28 T3, Arch Chemical Inc., Norwalk, CT) was applied on each substrate. The photoresist was spread at 600 rpm for 15 s and

spinned at 4000 rpm for 40 s. The substrates were then soft-baked at 90 °C for 5 minutes. The coated substrate was exposed to UV light for 3 s through a chrome lithographic mask. The mask contained a pattern of open squares (25 × 25 μm squares separated by 5 μm). The photoresist was developed with WNRD developer (Arch Chemical Inc., Norwalk, CT) for 45 s and rinsed with Rinse 1 (Arch Chemical Inc.) for 15 s. Finally each substrate was rinsed with deionized water, dried with nitrogen gas and then inspected under the microscope for pattern transfer.

Electrochemical Procedures. Both patterned and non-patterned ECF electrodes were modified with phenyl layers by carrying out cyclic voltammetry of the corresponding diazonium salt. Cyclic voltammetric experiments were performed in a standard three-electrode cell connected to a computer controlled bipotentiostat (Model AFCBP1; Pine Instruments Company). Data was recorded with Pine Chem (version 2.7.9) software. A Ag/AgCl/KCl (sat.) reference electrode and a platinum wire auxiliary electrode were used. The electrode area of the ECF (working) electrode was defined by an elastomeric O-ring (geometric area = 0.28 cm²). The scan rate was 100 mV/s for all voltammograms. After modification, the patterned ECF electrode was sonicated in xylene for 15 minutes to remove the remaining photoresist. Non-patterned ECF electrodes were sonicated in 50/50 2-propanol / acetonitrile (v/v) mixture for 10 minutes then rinsed with Nanopure water and dried with a stream of argon before using in electrochemical modification experiments.

Chronoamperometry experiments were carried out using the same bipotentiostat instrument. A GC disk electrode with a diameter of 3.0 mm, imbedded in a rod of teflon was used as the working electrode. The reference and auxiliary electrodes were same as those used in cyclic voltammetric experiments. The GC disk electrode was initially prepared by polishing successively in 1, 0.3, 0.05 μm alumina slurries in nanopure water (18 M Ω -cm) on polishing microcloth (Buehler). The electrode was sonicated in deionized water for 5 min between polishing steps.

AFM Imaging. Atomic Force Microscopy (AFM) was carried out using a Nanoscope IIIa Multimode microscope with Extender module for phase imaging (Digital Instruments, Santa Barbara, CA). Images were collected both in contact and tapping mode. Tapping mode imaging was performed with noncontact Si cantilevers (NSC 15/50, Ultrasharp) operating at 330-360 kHz. Images were collected at minimum force and the scan rate was usually ~ 1 Hz. For contact mode imaging, silicon nitride cantilevers (Nanoprobes, Digital Instruments) with nominal spring constants of 0.06 and 0.12 N/m were used. All images were collected in ambient air environment. Topographic images were flattened with a third order polynomial before analysis.

Results and Discussion

Aryl films formed on e-beam deposited carbon film (ECF) electrodes were probed using AFM. The surface morphology of unmodified ECF substrates (50 nm carbon film thickness) was first studied with AFM. Figure 3.1A shows the 8 \times 8

μm topographic contact-mode image of an unmodified ECF substrate. The image shows a smooth topography with no observable features. The root mean square (rms) roughness value of this image is 0.25 nm, in agreement with previous measurements from our group [17]. The ECF substrates used in this study had an average rms roughness of 0.30 ± 0.05 nm.

The ECF surface was next modified with a 4-nitrophenyl film by electrochemical reduction of 2.5 mM NB in CH_3CN (0.1M Bu_4NBF_4). Two potential cycles were carried out from +0.6 to -0.1 V vs. Ag/AgCl to affect the deposition. An example of a cyclic voltammogram for this deposition on ECF surface is shown in Figure 3.2A. The peak potential (E_p) and peak current (i_p) at ECFs ($E_p=0.16$ V, $i_p=116$ μA) are similar to that at GC ($E_p=0.16$ V, $i_p=108$ μA). This implies that the electrochemical reactivity for ECFs toward diazonium reduction is sufficient for aryl film formation. The modified ECF substrate was sonicated in CH_3CN for 10 minutes and dried with argon before AFM imaging. Figure 3.1B is a 8×8 μm tapping mode (TM) topographic image of the modified ECF substrate. The morphology of the 4-nitrophenyl (NP) film is somewhat porous and much less uniform than the initial ECF surface. The rms roughness of this surface is 1.12 nm. Although a change in morphology is observed after deposition of NP film, information on film thickness can not be gained by studying images like that of Figure 3.1B.

Our goal here is to measure the thickness of aryl layers and to investigate the effect of deposition medium and deposition cycles in the formation of these layers. The use of lithographically patterned ECF substrate provides a suitable

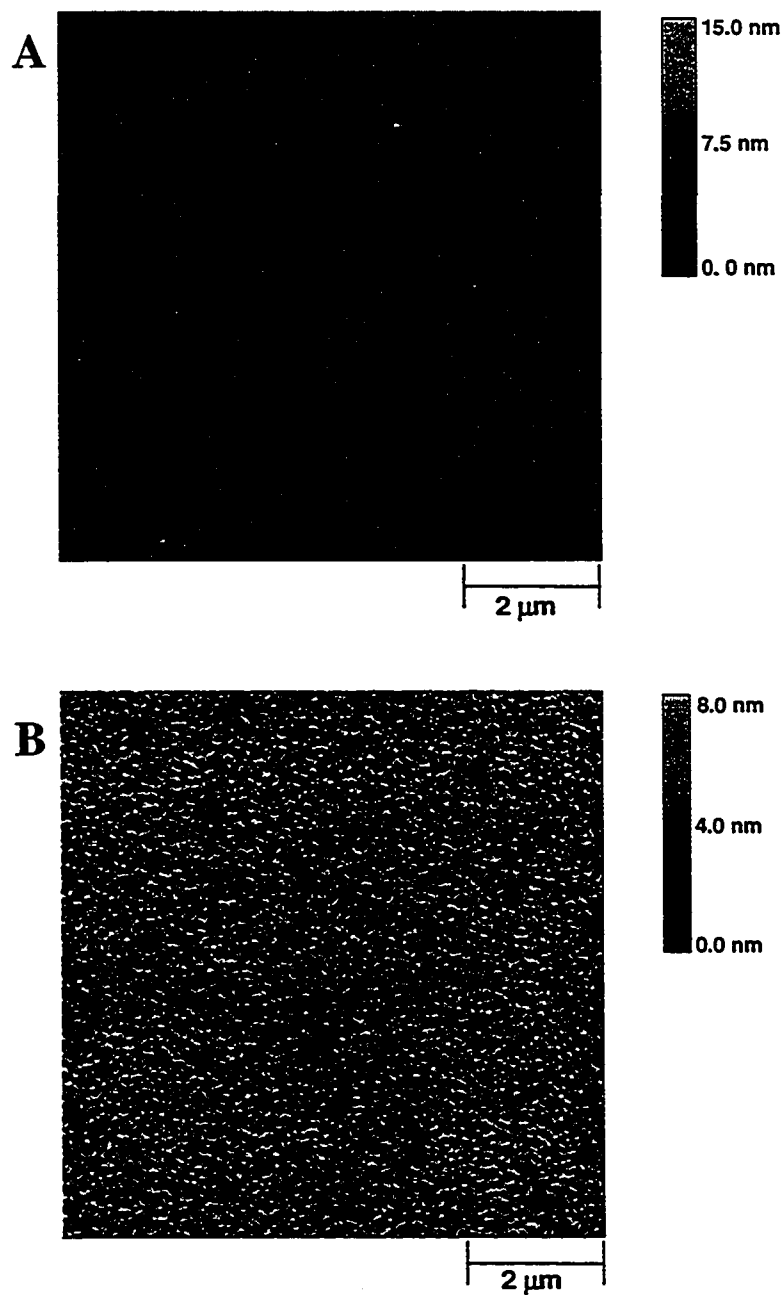


Figure 3.1: (A) 8 X 8 μm contact mode topographic image of an unmodified ECF substrate; rms roughness= 0.25 nm. (B) 8 X 8 μm tapping mode topographic image of an ECF substrate modified by two potential cycles in 2.5 mM NB(0.1M Bu₄NBF₄+ CH₃CN); rms roughness= 1.12 nm.

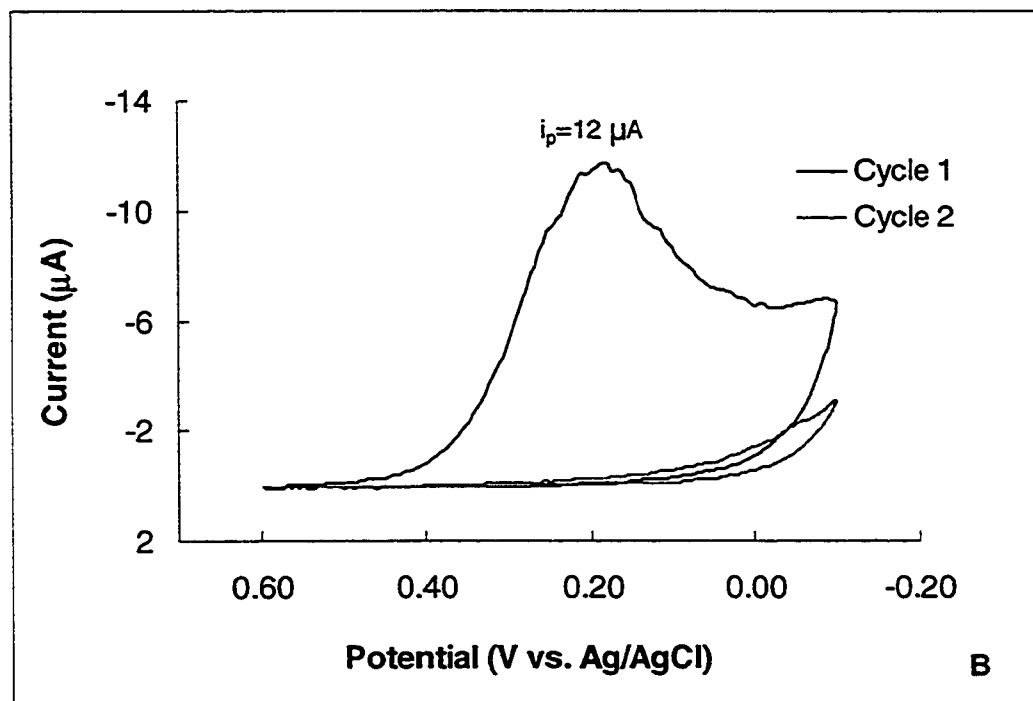
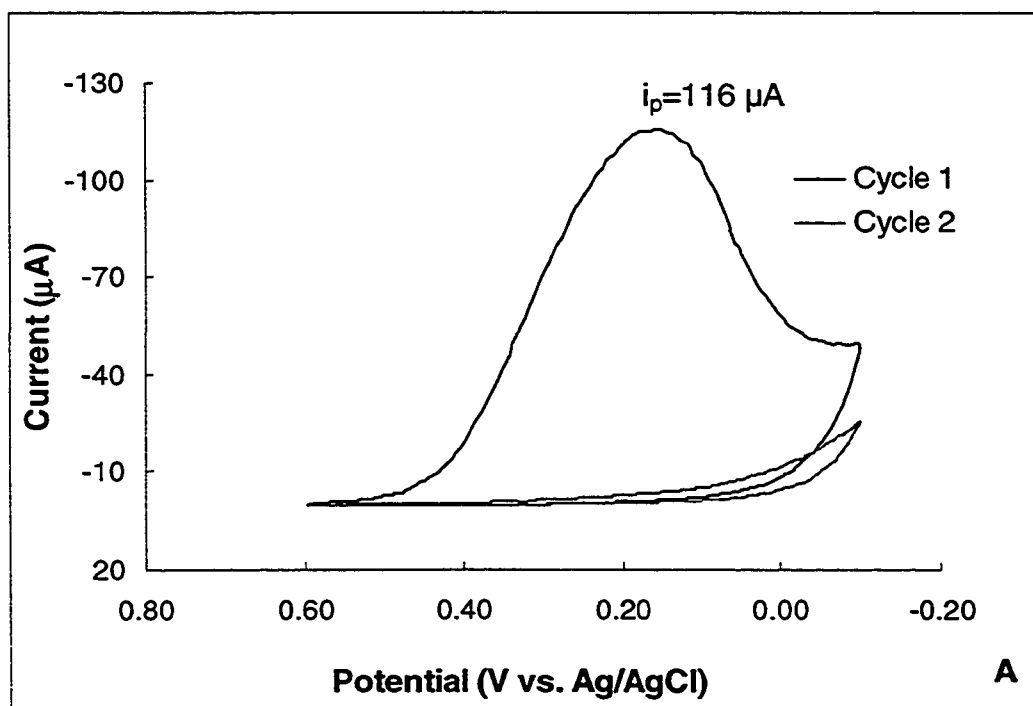


Figure 3.2: Cyclic voltammograms for the reduction of 2.5 mM NB from (0.1 M $\text{Bu}_4\text{NBF}_4 + \text{CH}_3\text{CN}$) on (A) unpatterned (B) patterned ECF surface.

means to achieve this goal. In a patterned ECF substrate, parts of the surface are covered with photoresist. When this substrate is used for electrochemical deposition, aryl layers are formed only on bare carbon surfaces. For example, also shown in Figure 3.2B is a voltammogram for the deposition of NP film on a patterned surface. The peak current ($i_p = 12 \mu\text{A}$) is substantially lower than that of the unpatterned electrode ($i_p = 116 \mu\text{A}$) due to the blocking by the lithographic pattern. After the modification, the photoresist layer is removed from the surface by sonication in xylene. The resulting substrate contains areas where aryl layers are formed and areas of unmodified carbon. This provides us with a surface, where thickness measurements with AFM become more reliable.

Figure 3.3 shows tapping mode images of a patterned ECF substrate modified with 2.5 mM NB in 0.1 M H_2SO_4 . The surface was modified by applying 2 potential cycles from +0.5 to -0.1 V vs. Ag/AgCl. The topographic image in Figure 3.3A clearly shows the square shaped pattern and contrast in heights between the NP film (higher topography) and unmodified ECF surface resulting from the patterning procedure. The films appear to form a compact layer of uniform height. Note that the films appear to be of lower height in the X direction, which is an effect of the flattening procedure and was absent in unflattened images. Part B of Figure 3.3 shows the corresponding tapping mode phase image. The higher topographical features exhibit a higher phase contrast. The observed contrast is generated as a result of phase angle shifts ($\Delta\phi$) between the oscillating cantilever and the driving signal as the tip interacts with the surface. Since the phase lag reflects the interactions between the scanning tip and the

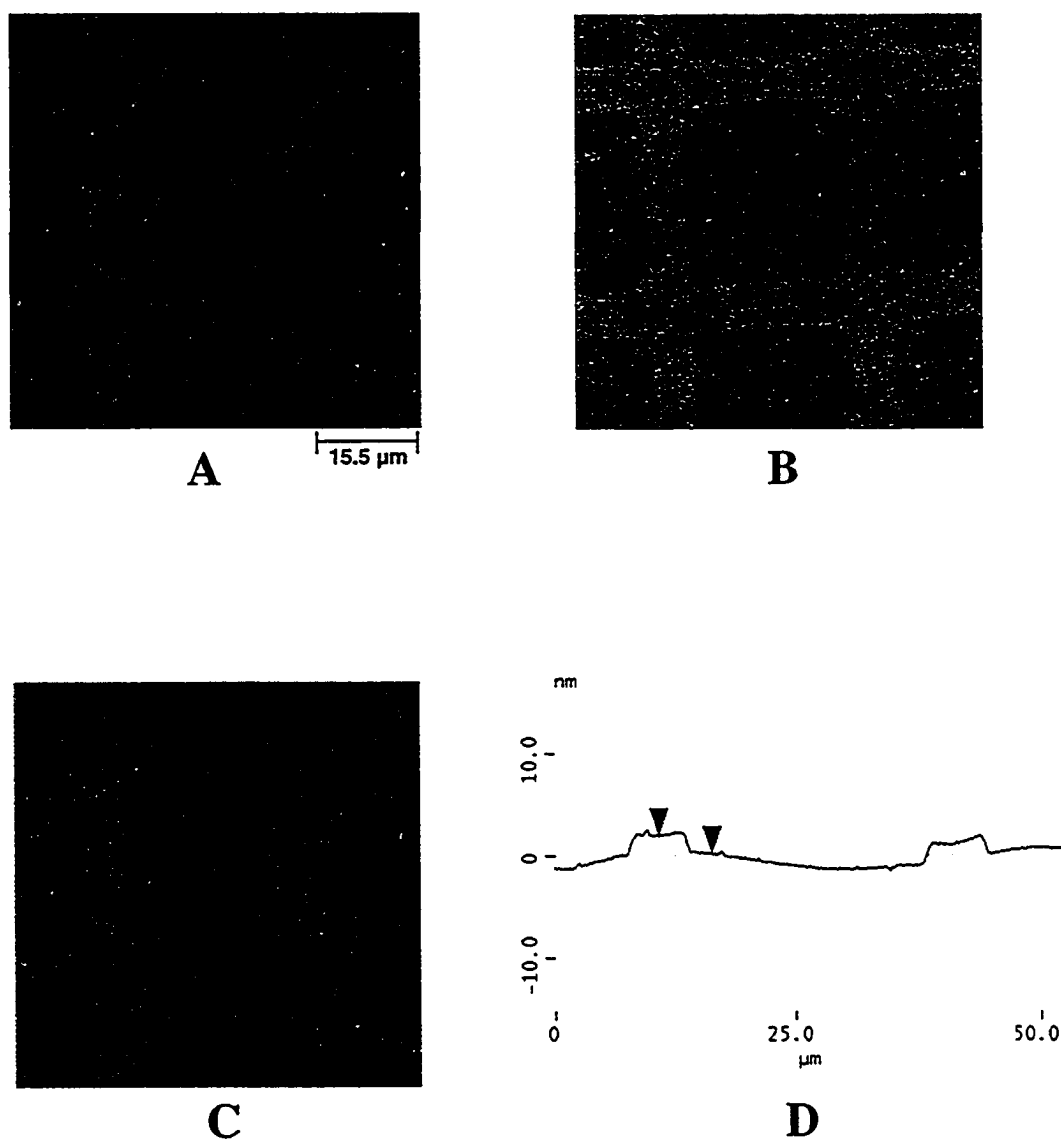


Figure 3.3: 62 X 62 μm tapping mode images of a patterned ECF substrate modified by 2 cycles in 2.5 mM NB(0.1 M H_2SO_4). (A) Topographic image, z scale= 30 nm (B) Phase contrast image, z scale= 150° (C) Average section analysis performed on the topographic image (D) Corresponding cross-sectional profile (aryl layer thickness= 1.74 nm).

sample surface, phase images can produce chemical maps of surfaces [19]. Figure 3.3B clearly shows the difference in surface composition between the aryl film and the underlying ECF substrate.

The thickness of NP layer was measured from average cross sectional profiles as shown in Figure 3.3D. A number of thickness measurements (at least 6) were made at different locations of the substrate and the arithmetic mean of these measurements are reported in Table 3.1. The average thickness of NP layer deposited from 0.1 M H_2SO_4 is 1.51 nm. The theoretical height of a nitrophenyl group standing up on a surface is 0.68 nm [20]. Hence, the NP film thickness obtained here is more than 2 layers. Next, a patterned ECF substrate was modified with 4 deposition cycles of 2.5 mM NB in 0.1 M H_2SO_4 . The average thickness was found to be 2.47 nm, which is close to 3.5 layers. This indicates that aryl films deposited from aqueous (0.1 M H_2SO_4) medium continue to grow with the number of deposition cycles.

The NP films deposited from aqueous solution (0.1 M H_2SO_4) were compared with those deposited from organic solution (0.1 M $\text{Bu}_4\text{NBF}_4 + \text{CH}_3\text{CN}$). Patterned ECF substrates were modified with 2 and 10 deposition cycles of 2.5 mM NB in 0.1 M $\text{Bu}_4\text{NBF}_4 + \text{CH}_3\text{CN}$. Figure 3.4A is a tapping mode topography image of a patterned ECF substrate modified with 10 deposition cycles of NB (0.1 M $\text{Bu}_4\text{NBF}_4 + \text{CH}_3\text{CN}$). The film thickness appears to be higher along the edge of the pattern. When thickness measurements were made, the vertical distance between the center of the aryl film and bare ECF substrate was

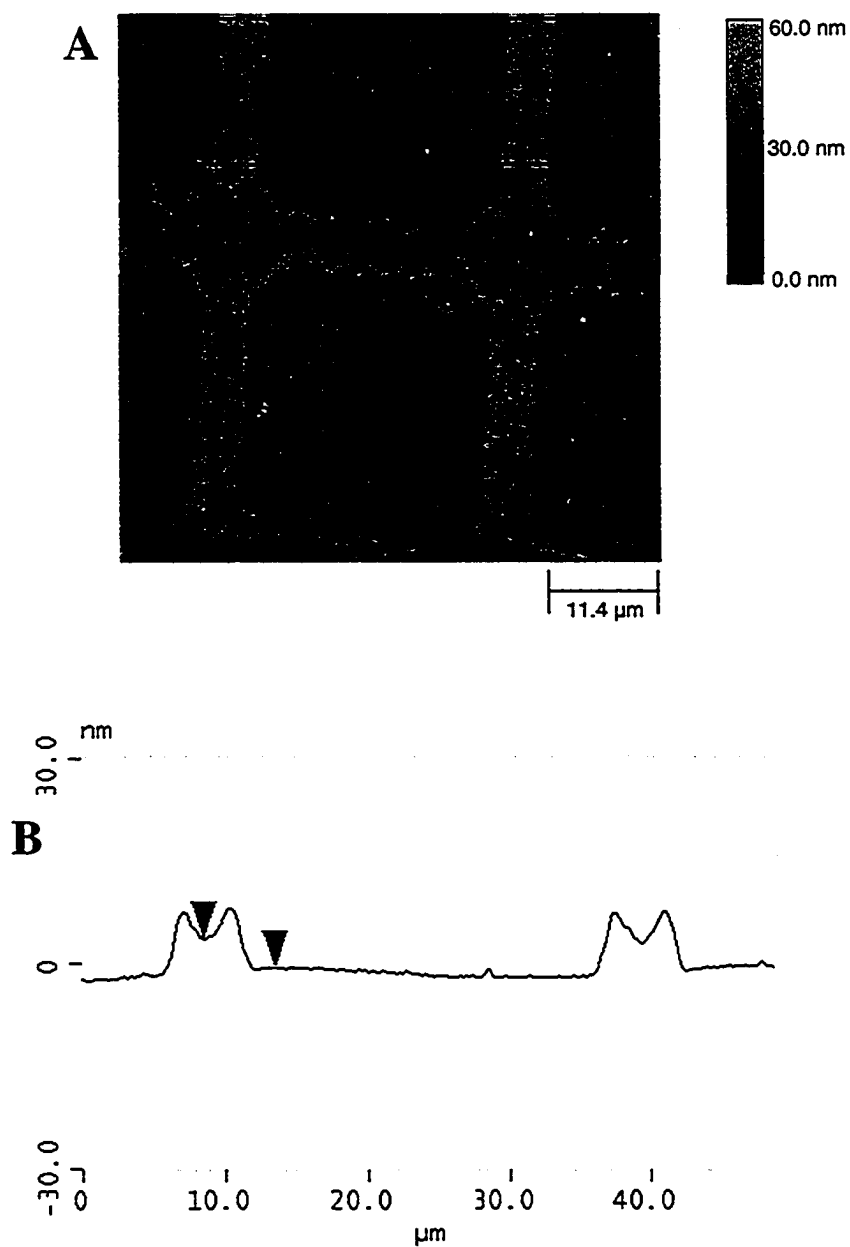


Figure 3.4: (A) 57 X 57 μm topographic AFM image of a patterned ECF substrate modified with 10 deposition cycles in 2.5 mM NB(0.1M Bu_4NBF_4 + CH_3CN) (B) Cross-sectional profile, aryl layer thickness= 4.22 nm.

measured (Figure 3.4B). The average thickness of nitrophenyl layer is 4.30 nm in this case.

The average film thicknesses for all films studied are listed in Table 3.1. The film thickness obtained from 2 deposition cycles in CH_3CN is 2.66 nm and is close to 4 layers. This is much higher than that obtained for deposition from aqueous acid solution under the same condition. Brooksby and Downard also found that NP_{AQ} films have a lower average thickness than NP_{ACN} films [15]. They suggested that nitrophenyl films resulting from modification in aqueous acid are inherently more blocking toward diazonium reduction than those formed in acetonitrile solution.

As indicated in Table 3.1, NP films are thicker when formed from CH_3CN compared to aqueous solutions. To explore the generality of this observation, biphenyl films were examined. Patterned ECF electrodes were modified by electrochemical reduction of 1 mM BP in both aqueous (0.1 M H_2SO_4) and organic (0.1 M $\text{Bu}_4\text{NBF}_4 + \text{CH}_3\text{CN}$) solutions. 2 deposition cycles were carried out from +0.6 to -0.6 V vs. Ag/AgCl. Figure 3.5 is a $34.5 \times 34.5 \mu\text{m}$ tapping mode image of a patterned ECF substrate, modified with 2 deposition cycles of BP in CH_3CN (0.1 M Bu_4NBF_4). Part A is the topographic and part B is the corresponding phase contrast image. The phase image shows clear contrast between the aryl layer and unmodified ECF substrate indicating their compositional difference. Figure 3.6A and B shows higher magnification topographic images of the biphenyl film. Apparent in Figure 3.6B, the BP film consists of regions exhibiting two different heights. The higher (brighter) domains

Precursor	Deposition Cycles	Average Thickness (nm)	Std. Dev.	No of Measurements
NB (0.1M Bu ₄ NBF ₄ + CH ₃ CN)	2	2.66	0.39	8
	10	4.30	0.80	12
NB (0.1M H ₂ SO ₄)	2	1.51	0.30	6
	4	2.47	0.46	6
BP (0.1M Bu ₄ NBF ₄ + CH ₃ CN)	2	4.70	0.73	8
BP (0.1M H ₂ SO ₄)	2	1.90	0.49	6

Table 3.1: Average thickness of electrochemically deposited aryl layers measured with AFM.

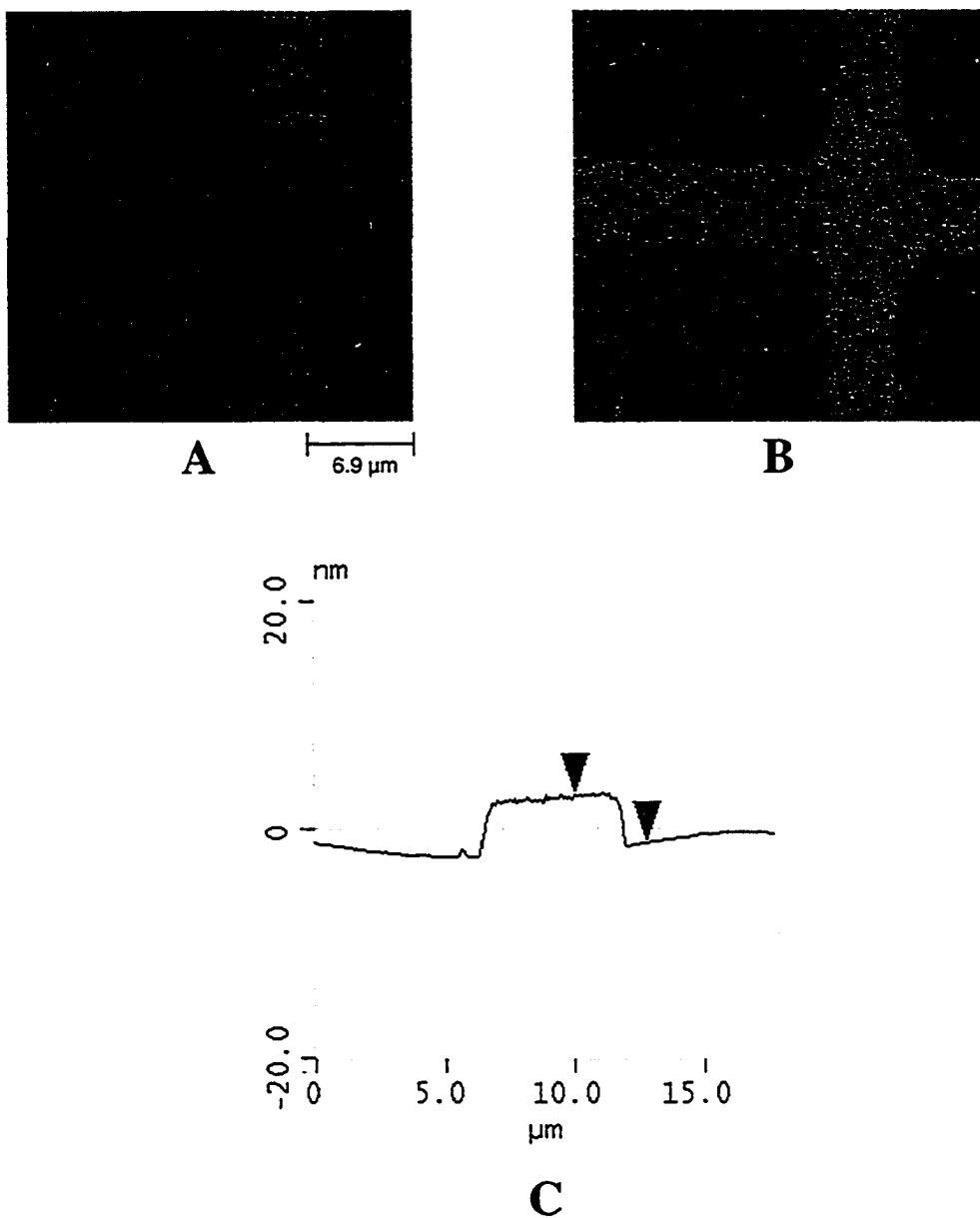


Figure 3.5: Tapping mode AFM images of a patterned ECF substrate modified by 2 cycles in 1 mM BP(0.1M $\text{Bu}_4\text{NBF}_4 + \text{CH}_3\text{CN}$). (A) Topographic image, z scale= 40 nm (B) Corresponding phase contrast image, z scale= 80° (C) Cross-sectional profile (aryl layer thickness= 4.20 nm).

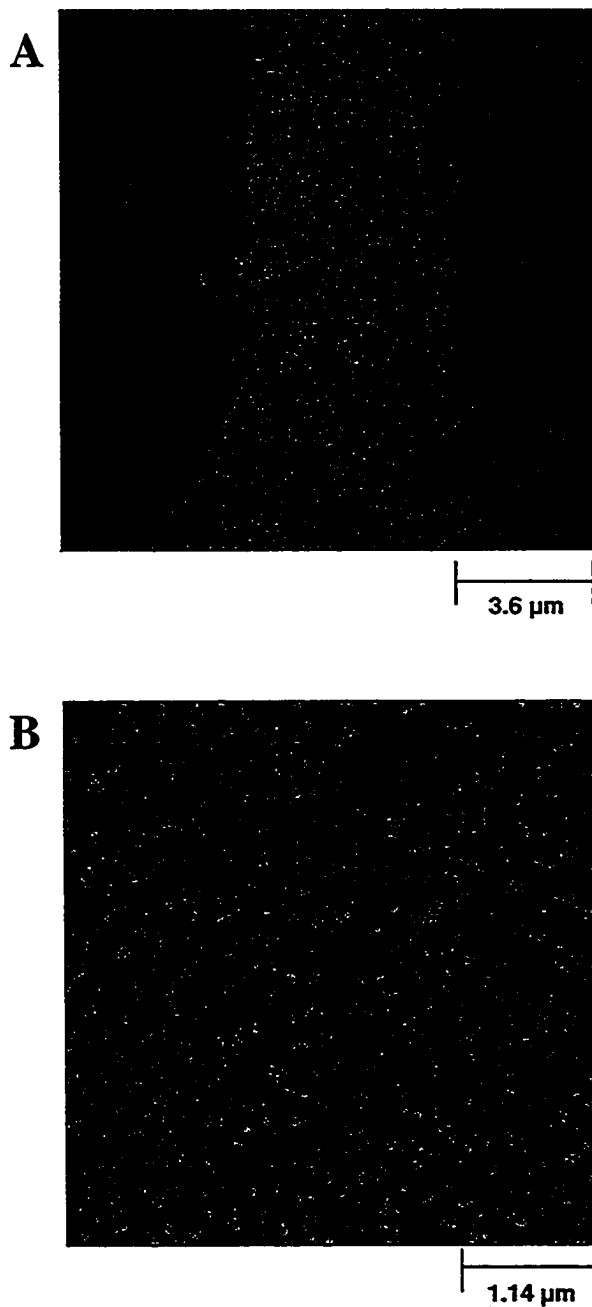


Figure 3.6: (A) 14.4 X 14.4 μm topographic AFM image of a patterned ECF substrate modified by 2 cycles in 1 mM BP (0.1M Bu₄NBF₄ + CH₃CN), z scale= 40 nm (B) A higher magnification image of the biphenyl film, z scale= 8 nm.

are ~ 3.21 nm above the lower domains. We believe the higher domains are areas where multilayer growth was more favorable. The average film thicknesses of biphenyl layers deposited from aqueous (BP_{AQ}) and organic solution (BP_{ACN}) are listed in Table 3.1. The theoretical length of 4-biphenyl group bonded perpendicularly to the carbon surface is 1.11 nm [14]. The thickness of BP_{ACN} is 4.70 nm, which is more than 4 layers. On the other hand the thickness of BP_{AQ} is 1.90 nm, which is less than 2 layers. These results have similarity with that obtained for nitrophenyl films. Anariba and coworkers measured the BP_{ACN} film thickness by using 'AFM scratching' method [14]. They reported BP_{ACN} film thickness after 1 and 4 derivatization scans as 1.51 and 1.71 nm respectively. These values are significantly lower than our measurements, which can be attributed to the different measurement techniques.

The results presented here indicate that the ability of electrochemically deposited aryl layers to form thick, multilayer films is greater in ACN solutions than aqueous H₂SO₄. To further explore this observation we compared the deposition voltammograms of NB on ECF in ACN and H₂SO₄. As shown in Figure 3.7 we observed about 3 times higher peak current when diazonium salts are deposited from organic medium in comparison to deposition from aqueous acid medium. On polished GC, peak current was on average 2 times higher for deposition from CH₃CN than aqueous acid solutions. The peak current in a cyclic voltammogram is given by [21]

$$i_p = (2.69 \times 10^5) n^{3/2} A D^{1/2} C^* \nu^{1/2} \quad (3.1)$$

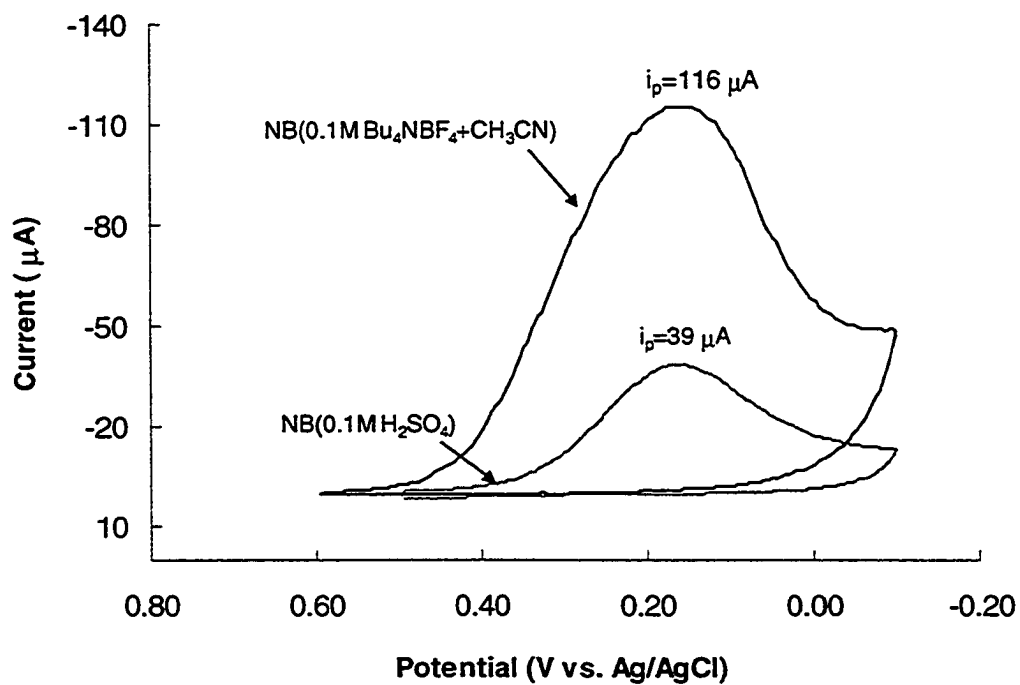


Figure 3.7: Comparison of peak current for the deposition of 2.5 mM NB from aqueous and organic medium on ECF surface. The electrode area for both measurements was 0.28 cm².

where n is the number of electrons, A is the electrode area (cm^2), D is the diffusion coefficient (cm^2/s) of the electroactive species, C^* is the bulk concentration (mol/cm^3) and v is the voltammetry scan rate (V/s). The voltammograms of Figure 3.7 led us to investigate the diffusion coefficient of diazonium salts, as all other factors affecting peak current (i.e. n , A , C^* and v) were same in both depositions.

We carried out chronoamperometry (potential step) experiments to measure the diffusion coefficient of NB in aqueous and organic solutions. The reduction peak potential of NB in both solutions is about 0.16 V. Hence the potential was stepped from +0.6 V to a final potential of -0.4 V and held for 5 s. The results (current vs. time plot) obtained from chronoamperometry of 2.5 mM NB in aqueous and organic medium is shown in Figure 3.8. An expression for diffusion limited current is obtained from Cottrell Equation [22],

$$i_D = \frac{nFAC^*D^{1/2}}{(\pi t)^{1/2}} \quad (3.2)$$

where, n is the number of electrons involved in reduction, F is Faraday's constant, A is electrode area, C^* is bulk concentration, D is diffusion coefficient and t is time. Hence a plot of i_D vs $t^{-1/2}$ should be linear with a slope (m),

$$m = \frac{nFAC^*D^{1/2}}{(\pi)^{1/2}} \quad (3.3)$$

Figure 3.9 shows the result of such a plot for electrolysis of NB in organic and aqueous acid medium. The current values from 33 ms to 99 ms are plotted to avoid the interference of double layer charging current at lower times and the effect of a changing electrode surface due to aryl film formation at longer times.

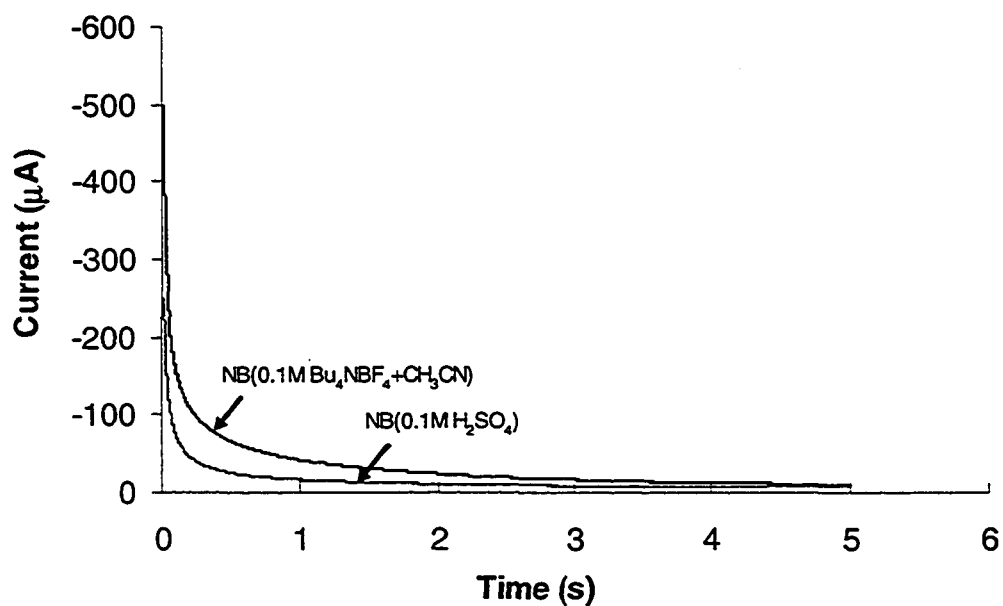


Figure 3.8: Electrolysis experiment of NB in aqueous and organic medium.

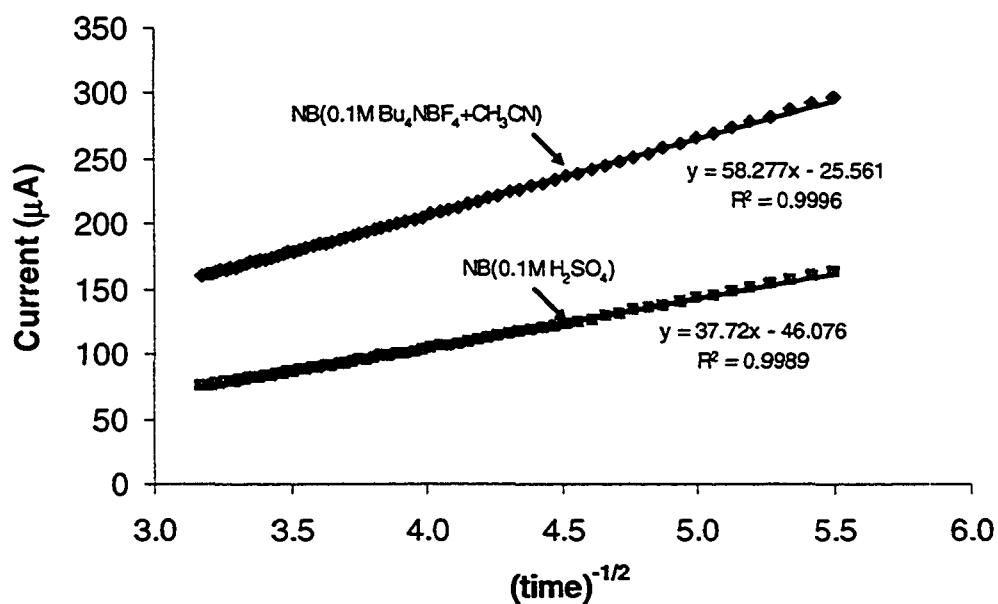


Figure 3.9: Current vs. $t^{-1/2}$ plot for electrolysis of NB in organic and aqueous acid medium. The symbols are the data points and the solid lines are the linear least-square fit. The equations for each linear fit are listed in the figure along with the square of the correlation coefficient (R^2).

Note from equation 3.2 that a plot of I vs. $t^{-1/2}$ should have a y-intercept of 0. The equations of the linear least fits listed in Figure 3.9 contain negative, non-zero intercepts. We believe this is due to the formation of the aryl film during the chronoamperometry experiment. The currents observed at longer times are likely lower than theory due to the blocking of the aryl layers.

The ratio of the two slopes can be expressed as,

$$\frac{m_{ACN}}{m_{AQ}} = \frac{C_{ACN}^* D_{ACN}^{1/2}}{C_{AQ}^* D_{AQ}^{1/2}} \quad (3.4)$$

Taking the ratio of the slopes in Figure 3.9 and the bulk concentration of NB in each media ($C_{ACN}^*=2.5169$ mM and $C_{AQ}^*=2.5338$ mM), the ratio $(D_{ACN}/D_{AQ})^{1/2}$ is 1.56. Note that voltammetric peak current depends on $D^{1/2}$ (Equation 3.1), thus our analysis predicts that i_p in ACN should be 1.56 times higher than in aqueous H_2SO_4 . As noted above, we observe 2-3 times higher i_p in ACN. Although the difference in i_p is not completely accounted for, it is clear from our analysis that the diffusion coefficient for NB is higher in ACN than in aqueous H_2SO_4 . In addition, we believe that the value for $(D_{ACN}/D_{AQ})^{1/2}$ of 1.56 is an approximate value due to the formation of a blocking aryl layer during the chronoamperometry experiment. The higher diffusion coefficient in ACN leads to more aryl radicals generated during a voltammetric scan, producing higher peak currents and thicker films in ACN.

Several recent reports have shown that aryl layers will spontaneously adsorb from diazonium salt solutions. Stewart and coworkers reported the direct grafting of conjugated molecules from aryl diazonium salt solutions on Si, GaAs and Pd surfaces [23]. Adenier *et. al.* have shown that nitrophenyl groups will bind

to carbon and metal (Fe, Zn, Ni, Cu) surfaces without electrochemical induction [24]. The self-assembly of nitrophenyl groups is examined here with AFM. Patterned ECF substrates were immersed in 10 mL solution of 2.5 mM NB in (0.1 M $\text{Bu}_4\text{NBF}_4 + \text{CH}_3\text{CN}$) for periods of 1 hour and overnight. The beaker was covered with Al foil and kept in a refrigerator during the immersion period. After immersion, the substrate was sonicated in xylene for 15 minutes to remove the remaining photoresist. The sample was then rinsed with CH_3CN and dried thoroughly with argon. The substrates were examined with tapping mode AFM. Figure 3.10 is a topographic image of a patterned ECF substrate immersed in 2.5 mM NB(CH_3CN) solution for 1 hour. The image clearly shows that a self-assembled 4-nitrophenyl layer has formed, which has a higher topography than the surrounding ECF substrate. The film appears less uniform when compared to those formed via electrochemical deposition. Some holes are observed in the self-assembled aryl films in several places. These holes could arise due to the presence of photoresist spots, which were not developed during lithography or could be due to inactive sites present in the ECF substrate.

The AFM measured thicknesses of 4-nitrophenyl film formed via self-assembly are listed in Table 3.2. The average thickness for an immersion period of 1 hour in organic solution is 1.20 nm and for overnight immersion is 1.41 nm. Hence the growth of self-assembled film over time is not very significant. Films self-assembled from aqueous solutions were also explored. Figure 3.11 shows the tapping mode topographic image of a patterned ECF substrate immersed in 2.5 mM NB in 0.1 M H_2SO_4 solution overnight. The image shows similar features

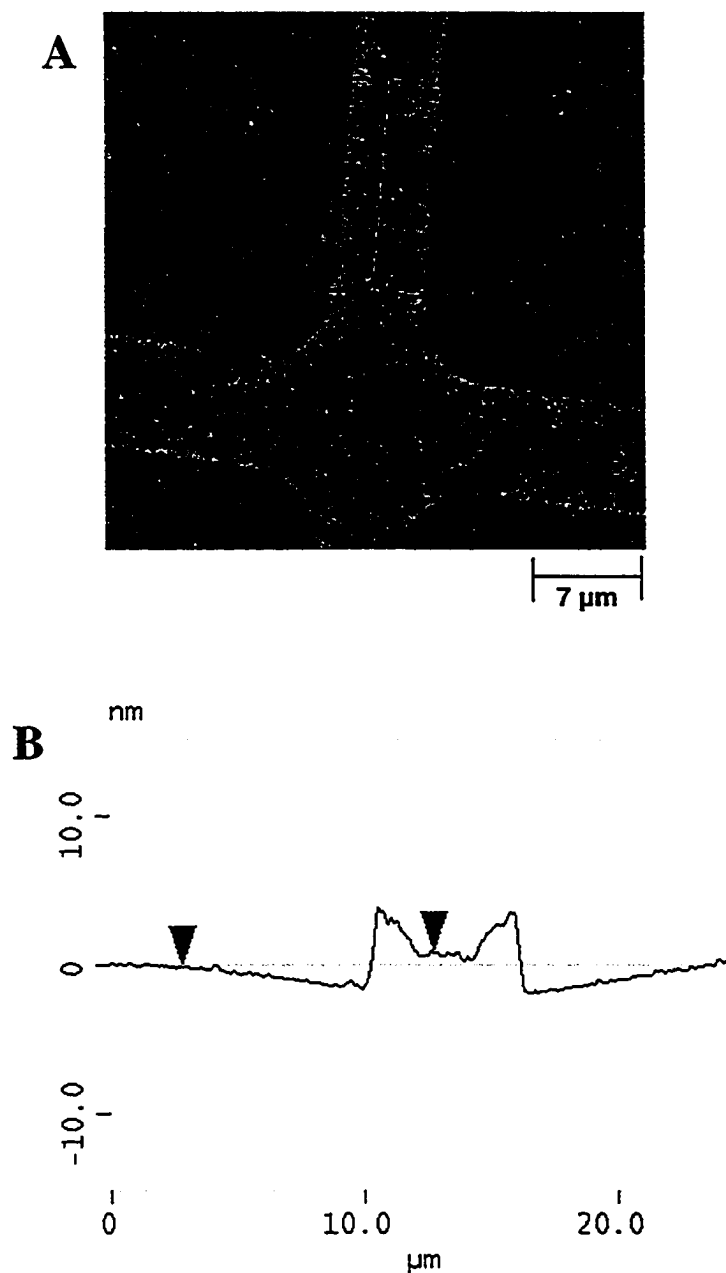


Figure 3.10: (A) 35 X 35 μm tapping mode topographic image of a patterned ECF substrate immersed in 2.5 mM NB((0.1M Bu_4NBF_4 + CH_3CN) for 1 hour, z scale= 30 nm (B) Cross-sectional profile (aryl layer thickness= 0.92 nm).

Precursor	Immersion Time	Average Thickness (nm)	Standard Deviation	No of Measurements
NB (0.1M Bu ₄ NBF ₄ + CH ₃ CN)	1 hour	1.20	0.39	4
	Overnight	1.41	0.40	8
NB (0.1M H ₂ SO ₄)	Overnight	1.30	0.54	8

Table 3.2: Average thickness of self-assembled nitrophenyl layers measured with AFM.

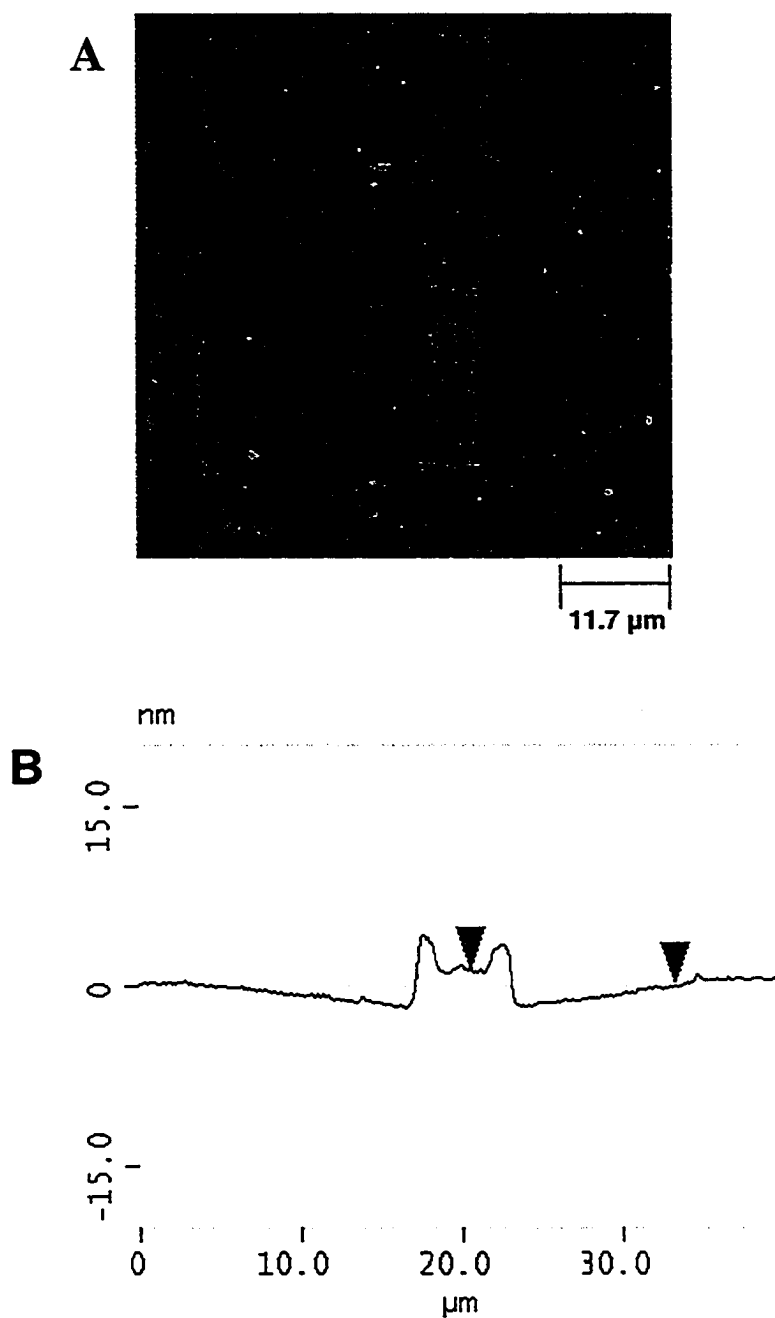


Figure 3.11: (A) Tapping mode topographic image of a patterned ECF substrate immersed overnight in 2.5 mM NB(0.1 M H₂SO₄), z scale= 40 nm (B) Cross-sectional profile (aryl layer thickness= 1.18 nm).

as that observed for self-assembled layers in CH₃CN solution. Importantly, this is the first evidence of aryl film self-assembly from diazonium salts in aqueous solutions. The average thickness is 1.30 nm, which is close to that obtained for overnight immersion in CH₃CN solution (1.41 nm). So in both cases, films are close to 2 layers thick. Recall that in the case of electrochemical deposition, the thicknesses of films obtained from CH₃CN solution were significantly higher than the ones from aqueous acid solution. The mechanism for the formation of self-assembled aryl layers from aryl diazonium salt on carbon surface is yet unknown. The key factor is the reduction of aryl diazonium salt to a reactive intermediate (aryl radical), in the absence of an applied potential. Stewart *et. al.* have reported a possible mechanism for the spontaneous activation of aryl diazonium salts to form covalently bound conjugated layers on hydride-passivated Si, GaAs and Pd surfaces [23]. They proposed a spontaneous electron transfer at the open circuit potential (OCP) of the substrate material in solution, leading to the local generation of aryl radicals by loss of N₂ and finally the formation of surface-molecule bonds.

Conclusions

Aryl films formed by electrochemical reduction of diazonium salts on carbon film electrodes were characterized with AFM. Patterned ECF electrodes were used as substrates, which provided a reliable means of measuring the thickness of aryl layers with TM-AFM. A minimum of two potential cycles were applied to modify the surface and this resulted multilayer formation of aryl films.

The thicknesses of substituted aryl films deposited from organic solution were higher than those deposited from aqueous acid solution. This may be due to the higher diffusion coefficient of diazoniums in CH₃CN, which results formation of more aryl radicals and greater thickness of aryl films in this medium. Self-assembled nitrophenyl films formed on carbon surface from both organic and aqueous acid solution. The thicknesses of the films obtained from both medium were comparable. The self-assembly of aryl groups from diazonium salt solutions on carbon and other conductive surfaces can lead to various practical applications. Further studies need to be carried out to ascertain the mechanism of formation and exact nature of these self-assembled aryl films.

References:

1. Delamar, M.; Hitmi, R.; Pinson, J.; Saveant, J.-M. *J. Am. Chem. Soc.* **1992**, *114*, 5883.
2. Allongue, P.; Delamar, M.; Desbat, B.; Fagebaume, O.; Hitmi, R.; Pinson, J.; Saveant, J.-M. *J. Am. Chem. Soc.* **1997**, *119*, 201.
3. Liu, Y.-C.; McCreery, R. L. *Anal. Chem.* **1997**, *69*, 2091.
4. Saby, C.; Oritz, B.; Champagne, G. Y.; Belanger, D. *Langmuir* **1997**, *13*, 6805.
5. Downard, A. J.; Roddick, A. D.; Bond, A. M. *Anal. Chim. Acta* **1995**, *317*, 303.
6. Dequaire, M.; Degrand, C.; Limoges, B. *J. Am. Chem. Soc.* **1999**, *121*, 6946.

7. De Villeneuve, C. H.; Pinson, J.; Bernard, M.-C.; Allongue, P. *J. Phys. Chem. B* **1997**, *101*, 2415.
8. Allongue, P.; De Villeneuve, C. H.; Cherouvrier, G.; Cortes, R.; Bernard, M.-C. *J. Electroanal. Chem.* **2003**, *550*, 161.
9. Adenier, A.; Bernard, M.-C.; Chehimi, M. M.; Cabet-Deliry, E.; Desbat, B.; Fagebaume, O.; Pinson, J.; Podvorica, F. *J. Am. Chem. Soc.* **2001**, *123*, 4541.
10. Bernard, M. C.; Chausse, A. Cabet-Deliry, E.; Chehimi, M. M.; Pinson, J.; Podvorica, F.; Vautrin-UI, C. *Chem. Mater.* **2003**, *15(18)*, 3450.
11. Kariuki, J. K.; McDermott, M. T. *Langmuir* **1999**, *15*, 6534.
12. Kariuki, J. K.; McDermott, M. T. *Langmuir* **2001**, *17*, 5947.
13. Ranganathan, S.; Steidel, I.; Anariba, F.; McCreery, R. L. *Nano Lett.* **2001**, *1*, 491.
14. Anariba, F.; Duvall, S. H.; McCreery, R. L. *Anal. Chem.* **2003**, *75*, 3837.
15. Brooksby, P. A.; Downard, A. J. *Langmuir* **2004**, *20*, 5038.
16. Brooksby, P. A.; Downard, A. J. *Langmuir* **2005**, *21*, 1672.
17. Blackstock, J. J.; Rostami, A. A.; Nowak, A. M.; McCreery, R. L.; Freeman, M. R.; McDermott, M. T. *Anal. Chem.* **2004**, *76*, 2544.
18. Solak, A. O.; Eichorst, L. R.; Clark, W. J.; McCreery, R. L. *Anal. Chem.* **2003**, *75*, 296.
19. Finot, M. O.; McDermott, M. T.; *J. Am. Chem. Soc.* **1997**, *119*, 8564.
20. Yang, H.-H.; McCreery, R. L. *Anal. Chem.* **1999**, *70*, 4081.

21. Bard, A. J.; Faulkner, L. R. In *Electrochemical Methods: Fundamentals and Applications*, John Wiley & Sons, 2001, p. 231.
22. Cottrel, F. G. *Z. Physik, Chem.* **1902**, *42*, 385.
23. Stewart, M. P.; Maya, F.; Kosynkin, D. V.; Dirk, S. M.; Stapleton, J. J.; McGuinness, C. L.; Allara, D. L.; Tour, J. M. *J. Am. Chem. Soc.* **2004**, *126*, 370.
24. Adenier, A.; Cabet-Deliry, E.; Chausse, A.; Griveau, S.; Mercier, F.; Pinson, J.; Vautrin-UI, C. *Chem. Mater.* **2005**, *17(3)*, 491.

Chapter IV

Conclusions and Future Work

Overall Conclusions

The aim of this research was to characterize aryl films formed by the reduction of diazonium salts from various aqueous solutions on carbon surfaces. Electrochemical and atomic force microscopy (AFM) measurements were used to investigate the nature of the films deposited from these mediums.

Glassy carbon (GC) and pyrolyzed photoresist film (PPF) electrodes were modified with NP films by electrochemical reduction of NB. Three different redox species, namely $\text{Fe}(\text{CN})_6^{3-/4-}$, $\text{Ru}(\text{NH}_3)_6^{3+/2+}$ and $\text{Eu}_{\text{aq}}^{3+/2+}$ were used to test the blocking ability of the resultant films. The films deposited from both aqueous acid and organic (0.1 M $\text{Bu}_4\text{NBF}_4 + \text{CH}_3\text{CN}$) solutions effectively blocked electron transfer to all three redox species. The blocking ability of the films, formed from both medium, was maximized after the first deposition cycle. The effect of pH of the deposition medium in the formation of aryl films was investigated with NB, PAA and BP diazonium salts. The aryl groups formed blocking films when deposited from acidic to neutral pH solutions. PAA was more soluble in aqueous solutions than the other diazonium salts and formed less blocking films than NB and BP. This suggests that solubility probably plays a role in film formation. Aryl films formed from basic solutions exhibited very little blocking ability. This is due to the fact that diazonium ions react chemically with basic solution and form a new species that do not form radicals electrochemically.

ECF electrodes were used as substrates for AFM study of aryl films. These carbon thin film (50 nm) electrodes show reasonable electrochemical activity and possess a near atomically smooth surface, which makes them an attractive substrate for AFM study. ECF electrodes were patterned by using standard photolithographic techniques. Next the patterned ECF electrodes were modified with aryl layers by applying a minimum of two potential cycles of the corresponding diazonium salt. The measurement of thickness of the resultant aryl films with TM-AFM revealed formation of multilayer films under this condition. The aryl multilayers could form via a polymerization type reaction between the bound monolayer and electrochemically generated radicals in solution [1].

The thickness of NP and BP films, deposited from organic solutions were higher than the films formed from aqueous acid solutions. This may be due to the higher diffusion coefficient of diazoniums in CH_3CN than in H_2SO_4 . Hence more radicals are formed from electrochemical reduction of diazoniums in CH_3CN , which generates films of higher thickness in organic medium. The self-assembly of aryl groups on ECF substrates from diazonium salt solutions was also investigated with TM-AFM. NP films self-assembled from CH_3CN and H_2SO_4 , were observed on carbon surface. The topography of these films appeared less uniform when compared to the electrochemically deposited films. The thickness of self assembled NP films formed from organic and aqueous acid solutions were reasonably close. This indicates that NP films formed from both mediums probably have similar structures. Self assembled aryl films on carbon surface

offers a promising area of research, which may find various practical applications, e.g. the area of molecular electronics.

Suggestions for Future Work

Our research has shown that functionalized aryl films can be deposited on carbon surfaces from aqueous acidic to neutral pH solutions by electrochemical reduction of the corresponding diazonium salts. However further work needs to be carried out to better understand the nature of these aryl films. Infrared reflectance absorbance spectroscopy (IRRAS) and Raman spectroscopy of modified electrode surface can provide important structural information of the surface bound species. These spectroscopic techniques have already been utilized to characterize aryl films formed from organic solutions [2-5] and can be compared to those deposited from aqueous solutions.

It would be interesting to study the formation of mixed monolayers on carbon surfaces. A recent report has described the nanoscale patterning of PPF surface with two chemical species by using 'AFM scratching' method [6]. Alternatively carbon surface patterned with photolithography can be used to graft aryl groups with a specific functional group. Then after removing the remaining photoresist from this modified substrate, aryl groups bearing a different functional group can be grafted on the same surface. These surfaces can be characterized with TM-AFM phase contrast images and may find application in the fabrication of sensors.

The self-assembly of NP films from aqueous and organic solutions on carbon surface was observed with AFM in Chapter III. Further work needs to be carried out to explore the direct grafting of other aryl groups from their corresponding diazonium salt solutions. Electrochemical studies can provide information on the blocking ability of these films. More research is also needed to ascertain the mechanism behind the formation of self assembled aryl layers on carbon surface.

References

1. Kariuki, J. K.; McDermott, M. T. *Langmuir* **1999**, *15*, 6534.
2. Liu, Y.-C.; McCreery, R. L. *J. Am. Chem. Soc.* **1995**, *117*, 11254.
3. Liu, Y.-C.; McCreery, R. L. *Anal. Chem.* **1997**, *69*, 2091.
4. Itoh, T.; McCreery, R. L. *J. Am. Chem. Soc.* **2002**, *124*, 10894.
5. Kariuki, J. K.; McDermott, M. T. *Langmuir* **2001**, *17*, 5947.
6. Brooksby, P.A.; Downard, A. J *Langmuir* **2005**, *21*, 1672.